Available online at www.sciencedirect.com
SCIENCE DIRECT®
International Journal of Solids and Structures 43 (2006) 4484–4508
INTERNATIONAL JOURNAL OF SOLIDS and STRUCTURES
www.elsevier.com/locate/ijsolstr

Spherically symmetric two-phase deformations and phase transition zones

A.B. Freidin [a,*], Y.B. Fu [b], L.L. Sharipova [a], E.N. Vilchevskaya [a]

[a] *Institute of Mechanical Engineering Problems, Russian Academy of Sciences, Bolshoy Pr. 61, V.O., St. Petersburg 199178, Russia*
[b] *Department of Mathematics, Keele University, Staffordshire ST5 5BG, UK*

Received 10 March 2005; received in revised form 25 October 2005
Available online 3 January 2006

Abstract

This paper is concerned with characterization and stability assessment of two-phase spherically symmetric deformations that can be supported by a nonlinear elastic isotropic material. We study general properties of equilibrium two-phase spherically symmetric deformations. Then we specialize to phase transformations of a solid sphere that is subjected to an all-round tension/pressure. Two material models are used to demonstrate a variety of transformation behaviours and some common features. For both materials we construct phase transition zones (PTZs) formed in the space of principal stretches by those which can exist adjacently to an equilibrium interface. Then we demonstrate how the PTZ can be used for the prediction of the number of two-phase spherically symmetric solutions and study how the deformation field associated with each solution is related to the PTZ. We show that even in the simplest case of one interface the solution is not unique: two equilibrium two-phase solutions as well as one uniform one-phase solution are found under the same boundary conditions. For the three solutions we construct their load-deformation diagrams and compare the associated total energies. The stability of the two-phase states with respect to radial and small-wavelength perturbations is also examined. We observe how unstable solutions are related with the PTZ.

Keywords: Phase transformations; Elastic sphere; Nonlinear elasticity; Stability

1. Introduction

If phase transformations take place in a deformable body, the interface between two different phases can be viewed as a singular surface across which the displacement is continuous but the deformation gradient suffers a discontinuity. Interfaces of this kind are called coherent interfaces and appear, for example, in martensite transformations. In contrast to deformations in a joint body where the interface between two materials is fixed, an additional jump condition (known as the Maxwell relation) needs to be added to conventional displacement and traction continuity conditions (see Grinfeld, 1980; James, 1981; Truskinovsky, 1982; Gurtin,

* Corresponding author.
E-mail address: freidin@mechanics.ipme.ru (A.B. Freidin).

0020-7683/$ - see front matter © 2005 Elsevier Ltd. All rights reserved.
doi:10.1016/j.ijsolstr.2005.10.008

1983; Abeyaratne, 1983; Kaganova and Roitburd, 1988; Fosdick and Hertog, 1989). This additional jump condition evolved from the pioneering works by Eshelby (1951, 1956, 1975), Ericksen (1975) and Knowles (1979). It acts as a restriction on the location and orientation of the interface.

Mathematical modelling of phase transformations consists of finding the right strain-energy function for a given material so that the theory can predict what will happen in various loading and geometrical conditions. The choice of the right strain-energy function is usually guided by results from a number of experiments such as uniaxial and biaxial tensions or twisting. It is now well-known that a necessary condition for an elastic body to support two-phase deformations is that its strain-energy function loses strong ellipticity at a non-trivial set of deformation gradients (see, e.g., Knowles and Sternberg, 1978). However, knowledge of such a necessary condition is far from enough in the mathematical modelling. A possible strategy is to study various two-phase deformations for as many strain-energy functions as possible so that a repertoire of basic transformation behaviours can be documented and then referenced in the construction of the strain-energy function for any particular situation. Thus, over the past three decades various two-phase deformations and boundary-value problems for elastic bodies capable of multi-phase deformations have been studied (see, for instance, James, 1979, 1981; Fosdick and James, 1981; Abeyaratne, 1981; Fosdick and MacSithigh, 1983; Eremeyev and Zubov, 1991; Fosdick and Zhang, 1993, 1994, 1995a,b; Abeyaratne et al., 2001), and the references therein. In the present paper we solve the boundary value problem of a solid sphere that is subjected to an all-round tension/pressure and consider the solution within the framework of phase transition zones (PTZs), formed in strain space by all deformations which can exist on either side of an equilibrium interface and determined entirely by the strain energy function (see Freidin and Chiskis, 1994a).

Aspects of phase transformations in a sphere made of nonlinear elastic or elastoplastic materials have previously been considered by Roitburd and Temkin (1986), Kaganova and Roitburd (1987), Lusk (1994), Levitas (1997, 2000). Our study is motivated by the following considerations.

Firstly, as a problem with an unknown interface, the problem of equilibrium two-phase deformations may have a number of solutions. Various two-phase structures can satisfy the equilibrium conditions under the same boundary conditions. Since equilibrium conditions do not necessarily provide a global energy minimum, some of the solutions may be metastable or unstable. The choice of the solution then needs to be made on the basis of analysis of stability and estimates of energy changes due to phase transformations. Note that not only are states which provide global energy minimum of interest, but locally stable states with different energies can also be observed in physical reality.

Secondly, recent studies by Morozov et al. (1996), Morozov and Freidin (1998), and Nazyrov and Freidin (1998) of phase transformations of an isotropic elastic sphere with a strain energy that is a piecewise quadratic function of the linear strain tensor show that (i) a new phase area can appear and spread during the loading either from the center of the sphere as a spherical nucleus or from the surface in the form of a spherical layer; (ii) for both solutions the external pressure decreases on the path of transformation when the volume of the sphere increases (strain softening); (iii) the equilibrium two-phase states, if they exist, are always energetically preferable to the one-phase state when radial displacement is prescribed; and (iv) with respect to radial perturbations of the interface both two-phase configurations are stable if displacement is prescribed but unstable if pressure is prescribed. Further examinations by Eremeyev et al. (2002, 2003, in press) have shown that a two-phase configuration in which the phase outside of the interface has a greater shear modulus is unstable with respect to spherically axisymmetric perturbations.

Thirdly, it has emerged from the above-mentioned studies that there might exist a connection between the stability properties of a two-phase configuration and the strain distribution in relation to the PTZ. Given an isotropic nonlinear elastic material, the PTZ may be constructed in the space of principal stretches. It has been found that corresponding to the unstable solution there are triads of principal stretches in the sphere that are inside the external PTZ boundaries, and instability was not found if the triad of principal stretches everywhere in the sphere is outside or on the external PTZ boundary.

In the present paper we study general properties of equilibrium spherically symmetric two-phase deformations of an arbitrary nonlinear elastic isotropic material. One of our objectives is to determine whether the results obtained in the case of small strains can be extended to finite deformations. We show the possibility of a finite spherical nucleus in an infinite medium or infinitesimally small nucleus at the center of a finite sphere. The deformation is spherical and axially symmetric inside and outside the nucleus, respectively, and

the principal stretches on the two sides of the interface are determined entirely by material properties and are obtained by solving the traction continuity condition and the Maxwell relation. The non-uniqueness of the two-phase deformation arises from the non-uniqueness of the solution of the latter equations. From the physical point of view, various solutions correspond to various phase states of the spherical nucleus. We show that the existence and number of solutions depend on the strain energy function and can be predicted a priori based on the PTZ constructed.

We demonstrate that for a phase-transforming elastic sphere a new phase area can spread from the center or from the outer surface of the sphere. We study the deformation fields in detail and show that unstable two-phase deformations are related to the PTZ in a similar manner to the case of small strains. We also obtain the relation between the applied pressure and the volumetric strain and show that it contains a decreasing branch on the path of phase transformation. This strain-softening effect in a sphere is similar to what was observed earlier in the case of small strains. Note that the existence of a decreasing branch in the average (macro) stress–strain relation is not a specific feature only of the phase-transforming sphere. Similar behaviour was also observed in the case of plane interfaces by Freidin (1997), Freidin and Sharipova (2003, in press), Idesman et al. (2004), Levitas et al. (2004).

The rest of this paper is organized into four sections as follows. In the next section we write down the jump conditions that need to be satisfied across any interface, define phase transition zones and show briefly how they can be constructed. In Section 3 we consider spherically symmetric two-phase deformations, particularly in the context of a solid sphere that is subjected to an all-round tension/pressure. We describe properties of equilibrium two-phase spherically symmetric deformations and reformulate for the case some results obtained by Sivaloganathan (1986) for cavitating equilibrium solutions. Then two material models are used to show a variety of phase transformation behaviours and some common features. For each material we show how the PTZ can be used to determine the two-phase deformation fields. In Section 4 we consider the stability of the two-phase solutions obtained in Section 3 with respect to small wave-length perturbations. In the final section we summarize our results.

2. Jump conditions and the phase transition zone (PTZ)

Let the static deformation of an elastic body be given by

$$\mathbf{x} = \mathbf{x}(\mathbf{X}), \tag{2.1}$$

which assigns position $\mathbf{x}$ to the material point that occupies position $\mathbf{X}$ in the undeformed (reference) configuration. Let Γ be a possible interface between two different phases in the undeformed configuration. Then the deformation must satisfy the jump conditions

$$[\![\mathbf{F}]\!] = \mathbf{f} \otimes \mathbf{m}, \quad [\![\mathbf{S}]\!]\mathbf{m} = \mathbf{0}, \quad [\![W]\!] = \mathbf{f} \cdot \mathbf{S}_{\pm}\mathbf{m} \tag{2.2}$$

which correspond to displacement continuity, traction continuity, and equilibrium of the interface (the Maxwell relation), respectively, where $\mathbf{F}$ is the deformation gradient, $\mathbf{f} = [\![\mathbf{F}]\!]\mathbf{m}$, W is the strain energy per unit reference volume, $\mathbf{S}$ is the first Piola–Kirchhoff stress tensor, the brackets $[\![\cdot]\!] = (\cdot)_+ - (\cdot)_-$ denote the jump of a function across Γ, super- or subscripts "$-$" and "$+$" signify evaluation at the interface as it is approached from the two sides, and $\mathbf{m}$ is the unit normal to Γ pointing from the "$+$" phase into the "$-$" phase. The stress tensor $\mathbf{S}$ is related to the Cauchy stress tensor $\mathbf{T}$ by $\mathbf{T} = J^{-1}\mathbf{S}\mathbf{F}^{\mathrm{T}}$, $J = \det\mathbf{F}$, and we have $\mathbf{S} = \partial W/\partial \mathbf{F}$ ($S_{ij} = \partial W/\partial F_{ij}$).

We may use $(2.2)_1$ to rewrite $(2.2)_{2,3}$ as

$$(\mathbf{S}(\mathbf{F}_- + \mathbf{f} \otimes \mathbf{m}) - \mathbf{S}(\mathbf{F}_-))\mathbf{m} = \mathbf{0},$$
$$W(\mathbf{F}_- + \mathbf{f} \otimes \mathbf{m}) - W(\mathbf{F}_-) = \mathbf{f} \cdot \mathbf{S}(\mathbf{F}_-)\mathbf{m}.$$

Given an $\mathbf{F}_-$, the above equations can be considered as a system of four equations for five unknowns: the amplitude $\mathbf{f} \neq \mathbf{0}$ and the unit normal $\mathbf{m}$. The *phase transition zone* (PTZ) is defined as the union of all those $\mathbf{F}_-$ for which the above system of equations have a real solution for $\mathbf{f}$ and $\mathbf{m}$ (see Freidin and Chiskis, 1994a). For isotropic materials, the PTZ can also be defined in terms of the three principal stretches or the three principal invariants of the Cauchy–Green deformation tensors.

A general procedure for constructing the PTZ for arbitrary isotropic nonlinear elastic materials has been developed earlier (see Freidin and Chiskis, 1994a,b; Freidin, 2000; Freidin et al., 2002). Here we summarize the main results which will be used in later sections.

When referred to the current configuration, the jump conditions (2.2) become

$$\mathbf{F}_+ = \left(\mathbf{I} + \frac{1}{J_-}\mathbf{c}\otimes\mathbf{n}\right)\mathbf{F}_-, \quad [\![\mathbf{T}]\!]\mathbf{n} = \mathbf{0}, \quad [\![W]\!] = \mathbf{c}\cdot\mathbf{T}_\pm\mathbf{n}, \tag{2.3}$$

where $\mathbf{n}$ is the unit normal to the interface in the current configuration, and $\mathbf{c} = J^\pm\mathbf{f}/\mid \mathbf{F}_\pm^{\mathrm{T}}\mathbf{n}\mid$ which is continuous across the interface. We decompose $\mathbf{c}$ such that

$$\mathbf{c} = [\![J]\!]\mathbf{n} + \mathbf{h}, \quad \mathbf{h} \triangleq \mathbf{P}\mathbf{c}, \tag{2.4}$$

where $\mathbf{P} = \mathbf{I} - \mathbf{n}\otimes\mathbf{n}$ is the projector, and in obtaining the first term we have used $(2.3)_1$. It then follows from $(2.3)_1$ and (2.4) that

$$\mathbf{B}_+ = \mathbf{B}_- + \frac{1}{J_-}(\mathbf{c}\otimes\mathbf{B}_-\mathbf{n} + \mathbf{B}_-\mathbf{n}\otimes\mathbf{c}) + G_1\mathbf{c}\otimes\mathbf{c}, \tag{2.5}$$

$$\mathbf{B}_+^{-1} = \mathbf{B}_-^{-1} - \frac{1}{J_+}(\mathbf{n}\otimes\mathbf{B}_-^{-1}\mathbf{c} + \mathbf{B}_-^{-1}\mathbf{c}\otimes\mathbf{n}) + \frac{1}{J_+^2}(\mathbf{c}\cdot\mathbf{B}_-^{-1}\mathbf{c})\mathbf{n}\otimes\mathbf{n}, \tag{2.6}$$

where $\mathbf{B} = \mathbf{F}\mathbf{F}^{\mathrm{T}}$ is the left Cauchy–Green tensor. The G_1 in (2.5), and G_{-1} which appears in our subsequent analysis, are the two orientation invariants defined by

$$G_1 = \frac{N_1}{J^2}, \quad G_{-1} = \frac{I_2}{J^2} - N_{-1}, \quad N_1 = \mathbf{n}\cdot\mathbf{B}\mathbf{n}, \quad N_{-1} = \mathbf{n}\cdot\mathbf{B}^{-1}\mathbf{n},$$

where I_1, I_2 are two of the three principal invariants of $\mathbf{B}$ related to the three principal stretches λ_1, λ_2, λ_3 by

$$I_1 = \lambda_1^2 + \lambda_2^2 + \lambda_3^2, \quad I_2 = \lambda_1^2\lambda_2^2 + \lambda_1^2\lambda_3^2 + \lambda_2^2\lambda_3^2.$$

It can be shown that G_1 and G_{-1} are both continuous across the interface (see, for instance, Freidin and Chiskis (1994a) or Freidin et al. (2002)).

When referred to the principal axes of stretch, the components of $\mathbf{n}$ can be determined in terms of G_1 and G_{-1} by solving the system of equations

$$\sum_{i=1}^{3} n_i^2 = 1, \quad \sum_{i=1}^{3} n_i^2\lambda_i^2 = J^2G_1, \quad \sum_{i=1}^{3} n_i^2\lambda_i^{-2} = \frac{I_2}{J^2} - G_{-1}, \tag{2.7}$$

which is linear in n_1^2, n_2^2 and n_3^2. Since n_1^2, n_2^2 and n_3^2 must be non-negative, the domain of admissible pairs of (G_1, G_{-1}) is a triangle $\mathscr{G}$ in the (G_1, G_{-1})- plane; see Fig. 1. The coordinates of the three vertexes A_1, A_2 and A_3 are given by

$$(\lambda_2^{-2}\lambda_3^{-2}, \lambda_2^{-2} + \lambda_3^{-2}), \quad (\lambda_1^{-2}\lambda_3^{-2}, \lambda_1^{-2} + \lambda_3^{-2}), \quad (\lambda_2^{-2}\lambda_1^{-2}, \lambda_2^{-2} + \lambda_1^{-2}),$$

respectively. For an isotropic material, we have

$$W = W(I_1, I_2, J), \quad \mathbf{T} = \mu_0\mathbf{I} + \mu_1\mathbf{B} + \mu_{-1}\mathbf{B}^{-1}, \tag{2.8}$$

where

$$\mu_0 = W_3 + 2J^{-1}I_2W_2, \quad \mu_1 = 2J^{-1}W_1, \quad \mu_{-1} = -2JW_2, \tag{2.9}$$

and $W_1 = \partial W/\partial I_1$, $W_2 = \partial W/\partial I_2$, $W_3 = \partial W/\partial J$. On substituting (2.4) into (2.5), (2.6) and making use of the equality $I_2 = J^2\,\mathrm{tr}\,\mathbf{B}^{-1}$, we obtain the following relations between the strain and orientation invariants

$$[\![I_1]\!] = G_1[\![J^2]\!] + 2\mathbf{h}\cdot\mathbf{t}_1^- + G_1\mathbf{h}\cdot\mathbf{h}, \tag{2.10}$$

$$[\![I_2]\!] = G_{-1}[\![J^2]\!] - 2\mathbf{h}\cdot\mathbf{t}_{-1}^- + \mathbf{h}\cdot\mathbf{B}^{-1}\mathbf{h}, \tag{2.11}$$

where

$$\mathbf{t}_1 = J^{-1}\mathbf{P}\mathbf{B}\mathbf{n}, \quad \mathbf{t}_{-1} = J\mathbf{P}\mathbf{B}^{-1}\mathbf{n}. \tag{2.12}$$

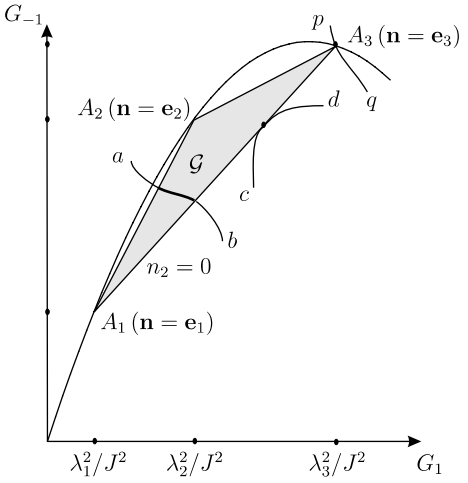

Fig. 1. The domain of admissible values of (G_1, G_{-1}). Lines ab, cd and pq: typical solutions of (2.19).

Projecting the traction continuity condition $(2.3)_2$ onto the normal direction and taking into account (2.8), (2.9) we obtain

$$-[\![W_3]\!] = 2[\![JW_1]\!]G_1 + 2[\![JW_2]\!]G_{-1}. \tag{2.13}$$

The Maxwell relation $(2.3)_3$ takes the form

$$[\![W]\!] = \tau_n[\![J]\!] + 2W_1^-\mathbf{h}\cdot\mathbf{t}_1^- - 2W_2^-\mathbf{h}\cdot\mathbf{t}_{-1}^-, \tag{2.14}$$

where τ_n is the normal component of the traction given by

$$\tau_n = \mathbf{n}\cdot\mathbf{T}\mathbf{n} = 2J(G_1W_1 + G_{-1}W_2) + W_3 \tag{2.15}$$

and can be evaluated on either side of the interface.

When projected onto the tangent direction, $(2.3)_2$ gives $\mathbf{P}[\![\mathbf{T}]\!]\mathbf{n} = \mathbf{0}$ which yields an equation for $\mathbf{h}$:

$$\mathbf{A}_+\mathbf{h} = -[\![W_1]\!]\mathbf{t}_1^- + [\![W_2]\!]\mathbf{t}_{-1}^-, \quad \mathbf{A}_+ \triangleq G_1W_1^+\mathbf{I} + W_2^+\mathbf{P}\mathbf{B}_\pm^{-1}. \tag{2.16}$$

We assume that the strong ellipticity condition, and hence the Baker–Ericksen inequalities $W_1 + \lambda_k^2 W_2 > 0$ $(k = 1, 2, 3)$, hold on both sides of the interface. Then the inverse of $\mathbf{A}_+$ exists (see Freidin, 2000) and $(2.16)_1$ can be solved to find an expression for $\mathbf{h}$. Following Freidin and Chiskis (1994a), we write

$$\mathbf{h} = \alpha\mathbf{t}_1^- + \beta\mathbf{t}_{-1}^-, \tag{2.17}$$

where the coefficients α and β are determined by the following matrix equation which results from substituting (2.17) into $(2.16)_1$ and then equating the coefficients of $\mathbf{t}_1^-$ and $\mathbf{t}_{-1}^-$:

$$\begin{pmatrix} G_1W_1^+ & W_2^+ \\ -G_1W_2^+ & G_1W_1^+ + G_{-1}W_2^+ \end{pmatrix}\begin{pmatrix}\alpha\\ \beta\end{pmatrix} = \begin{pmatrix} -[\![W_1]\!] \\ [\![W_2]\!]\end{pmatrix}. \tag{2.18}$$

Suppose that $I_1^-,\ I_2^-,\ J^-$ are prescribed. Then Eqs. (2.10), (2.11), (2.13), (2.14) together with the representation (2.17), (2.18) can be reduced to a system of four equations for five unknowns: the two orientation invariants G_1, G_{-1}, and the three deformation invariants $I_1^+,\ I_2^+,\ J^+$.

Suppose we solve three of the equations to express $I_1^+,\ I_2^+,\ J_+$ in terms of G_1 and G_{-1}. Then the fourth equation takes the form

$$\Psi(G_1, G_{-1}|I_1^-, I_2^-, J^-) = 0, \tag{2.19}$$

which describes a curve in the (G_1, G_{-1})-plane. The phase transition zone in the $(\lambda_1, \lambda_2, \lambda_3)$–space is formed by all triads of principal stretches at which the intersection between this curve and the triangular region in Fig. 1

is non-empty. The intersection may be a line segment, in which case we have a one-parameter family of solutions for the normal to the interface.

Since (G_1, G_{-1}) can only take values in $\mathscr{G}$, the PTZ is given by the following inequalities which can be used to construct the PTZ:

$$\Psi_{\min}(I_1, I_2, J) \leqslant 0 \leqslant \Psi_{\max}(I_1, I_2, J), \tag{2.20}$$

where

$$\Psi_{\min}(I_1, I_2, J) = \min_{G_1, G_{-1} \in \mathscr{G}} \Psi(G_1, G_{-1} | I_1, I_2, J),$$
$$\Psi_{\max}(I_1, I_2, J) = \max_{G_1, G_{-1} \in \mathscr{G}} \Psi(G_1, G_{-1} | I_1, I_2, J),$$

and we have omitted the superscripts "−" since the formulas are also valid for the "+" phase.

3. Spherically symmetric two-phase deformations

We now specialize to the case of a solid sphere that is subjected to an all-round tension or pressure. Without loss of generality, we may assume that the sphere has unit radius in its undeformed configuration. Suppose further that a spherical interface $R = R_*$ exists and divides the sphere into regions

$$V_{\text{in}} : R \in [0, R_*] \quad \text{and} \quad V_{\text{ex}} : R \in (R_*, 1].$$

We look for a solution whereby the deformations in V_{in} and V_{ex} are spherical and spherically symmetric, respectively. Thus, for $R \in V_{\text{in}}$ the deformation is uniform and we have

$$\mathbf{B} \equiv \mathbf{B}_- = \lambda_0^2 \mathbf{I}, \tag{3.1}$$

where $\lambda_0 > 0$ is a constant.

Assume that the material is strongly elliptic inside the phases including both sides of the interface. Then, since $\mathbf{t}_1 = \mathbf{t}_{-1} = \mathbf{0}$, from (2.17), (2.5) and (3.1) it follows that $\mathbf{h} = \mathbf{0}$, and $\mathbf{B}_+$ must necessarily take the form

$$\mathbf{B}_+ = \lambda_1^{*2} \mathbf{e}_1 \otimes \mathbf{e}_1 + \lambda_0^2 (\mathbf{I} - \mathbf{e}_1 \otimes \mathbf{e}_1), \tag{3.2}$$

where $\mathbf{e}_1$ is the base vector in the radial direction, and $\lambda_1^* > 0$ is a constant which, together with λ_0, is to be determined by

$$\left.\frac{\partial \tilde{W}}{\partial \lambda_1}\right|_{\lambda_1 = \lambda_2 = \lambda_3 = \lambda_0} = \left.\frac{\partial \tilde{W}}{\partial \lambda_1}\right|_{\lambda_1 = \lambda_1^*,\ \lambda_2 = \lambda_3 = \lambda_0} = \frac{\tilde{W}_+ - \tilde{W}_-}{\lambda_1^* - \lambda_0}, \tag{3.3}$$

where $\tilde{W}(\lambda_1, \lambda_2, \lambda_3) = W(I_1, I_2, J)$. The two equations above correspond to traction continuity and the Maxwell relation, respectively.

For $R \in V_{\text{ex}}$ we may write

$$r = r(R), \quad \theta = \Theta, \quad \phi = \Phi, \tag{3.4}$$

where R, Θ, Φ and r, θ, ϕ are spherical polar coordinates of material particles in the reference and current configurations, respectively. Corresponding to (3.4) the $\mathbf{F}$ and $\mathbf{B}$ are given by

$$\mathbf{F} = \lambda_1 \mathbf{e}_1 \otimes \mathbf{e}_1 + \lambda (\mathbf{I} - \mathbf{e}_1 \otimes \mathbf{e}_1), \quad \mathbf{B} = \lambda_1^2 \mathbf{e}_1 \otimes \mathbf{e}_1 + \lambda^2 (\mathbf{I} - \mathbf{e}_1 \otimes \mathbf{e}_1), \tag{3.5}$$

and the principal stretches are given by

$$\lambda_1 \equiv \lambda_R = r', \quad \lambda \equiv \lambda_\Phi = \lambda_\Theta = \frac{r}{R}, \tag{3.6}$$

where a prime denotes differentiation with respect to R.

The strain invariants are then given by

$$I_1 = r'^2 + 2\frac{r^2}{R^2}, \quad I_2 = \frac{r^2}{R^2}\left(2r'^2 + \frac{r^2}{R^2}\right), \quad J = r'\frac{r^2}{R^2}, \tag{3.7}$$

and the Cauchy stress tensor is

$$\mathbf{T} = \tau_1 \mathbf{e}_1 \otimes \mathbf{e}_1 + \tau(\mathbf{I} - \mathbf{e}_1 \otimes \mathbf{e}_1), \tag{3.8}$$

where

$$\tau_1 = \lambda^{-2} \frac{\partial \tilde{W}}{\partial \lambda_1}\bigg|_{\lambda_2=\lambda_3=\lambda}, \quad \tau = (\lambda_1 \lambda)^{-1} \frac{\partial \tilde{W}}{\partial \lambda_2}\bigg|_{\lambda_2=\lambda_3=\lambda}. \tag{3.9}$$

The equilibrium equations in spherical polar coordinates reduce to a single equation

$$\tau_1' + \frac{2r'}{r}(\tau_1 - \tau) = 0. \tag{3.10}$$

For the current deformation where $\lambda_2 = \lambda_3 \equiv \lambda$, we define a reduced strain energy function $\bar{W}$ through $\bar{W}(\lambda_1, \lambda) = \tilde{W}(\lambda_1, \lambda, \lambda)$. It then follows that

$$\frac{\partial \tilde{W}}{\partial \lambda_1} = \frac{\partial \bar{W}}{\partial \lambda_1} \triangleq \bar{W}_1, \quad \frac{\partial \tilde{W}}{\partial \lambda_2} = \frac{\partial \tilde{W}}{\partial \lambda_3} = \frac{1}{2}\frac{\partial \bar{W}}{\partial \lambda} \triangleq \frac{1}{2}\bar{W}_2,$$

and by (3.9), the equilibrium equation (3.10) reduces to

$$R\bar{W}_{11} r'' + \bar{W}_{12}\left(r' - \frac{r}{R}\right) + 2\bar{W}_1 - \bar{W}_2 = 0, \tag{3.11}$$

where $\bar{W}_{11} = \partial^2 \bar{W}/\partial \lambda_1^2$, $\bar{W}_{12} = \partial^2 \bar{W}/\partial \lambda_1 \partial \lambda$.

The second-order differential equation (3.11) is to be solved in the spherical shell $R \in [(R_*, 1]$ for

$$r \in C^2((R_*, 1]) : r'(R) > 0, \quad R_* \in (0, 1), \tag{3.12}$$

subjected to three conditions, namely the interfacial conditions

$$r(R_*) = R_* \lambda_0, \qquad r'(R_*) = \lambda_1^* \tag{3.13}$$

and the prescribed displacement condition

$$r(1) = r_0, \tag{3.14}$$

where r_0 is a constant which can be related to the applied pressure at $R = 1$. Note that (3.12) and $(3.13)_1$ assure $r(R) > 0$.

An equilibrium two-phase state of the sphere exists only for those values of r_0 at which the solution of (3.11) satisfies (3.12) and the two conditions (3.13) at a value of R_* in the interval $(0, 1)$. Suppose that λ_0 and λ_1^* are known and the solution $r(R)$ exists for all $R_* \in (0, 1)$ and as $R_* \to 0$. Then, given an interface $R_* \in (0, 1)$, one can integrate (3.11) from $R = R_*$ to $R = 1$ to obtain the required value of r_0 through $r_0 = r(1)$. As a result, the dependence of the interface radius R_* on the outer radius r_0 can be constructed.

If (3.3) has a number of solutions then every pair of positive numbers λ_0, λ_1^* produces an equilibrium spherically symmetric two-phase deformation.

Given a strain energy function, the solution $r(R)$, if it exists, and the dependence $R_*(r_0)$ can be obtained numerically. Examples in relation to phase transition zone for different nonlinear elastic materials are given in later subsections. Now we describe some general features of equilibrium spherically symmetric two-phase deformations.

3.1. Properties of the deformations at $R > R_*$

We first formulate some constitutive hypotheses. A necessary condition for the existence of spherically symmetric two-phase deformations is solvability of (3.3), i.e. $\tilde{W}$ must be such that at least one set of positive λ_0 and λ_1^* exists.

We assume that W is C^3, and strong ellipticity holds inside each phase. It then follows that

$$\bar{W}_{11} > 0, \quad \frac{\lambda \bar{W}_2 - 2\lambda_1 \bar{W}_1}{\lambda - \lambda_1} > 0, \tag{3.15}$$

$$\bar{W}_{12} + \frac{2\bar{W}_1 - \bar{W}_2}{\lambda_1 - \lambda} + (\bar{W}_{11}\bar{W}_{22})^{1/2} > 0 \tag{3.16}$$

at $\lambda_1 = r'(R)$, $\lambda = r(R)/R$, see Wang and Aron (1996). Note that since a material must loss ellipticity at some deformations, we cannot assume that (3.15) and (3.16) are satisfied at all principal stretches.

We observe that the second-order differential equation (3.11) may be rewritten as a first-order differential equation for $\lambda_1 = \lambda_1(\lambda)$:

$$\bar{W}_{11}\frac{\mathrm{d}\lambda_1}{\mathrm{d}\lambda} + \bar{W}_{12} + \frac{2\bar{W}_1 - \bar{W}_2}{\lambda_1 - \lambda} = 0, \tag{3.17}$$

We make the slightly stronger assumption

$$\bar{W}_{12} + \frac{2\bar{W}_1 - \bar{W}_2}{\lambda_1 - \lambda} > 0 \tag{3.18}$$

for each phase which, although in general not guaranteed by the strong ellipticity, is satisfied by the material models to be considered later.

By (3.13), the initial condition for (3.17) is

$$\lambda_1(\lambda_0) = \lambda_1^*. \tag{3.19}$$

Both the first-order differential equation (3.17) and the initial condition (3.19) are independent of R_*. Thus, the solutions for different values of R_* should be parts of a single curve that starts from the point (λ_0, λ_1^*) on the λ, λ_1-plane. This fact is borne out by our numerical calculations to be presented later.

After the solution $\lambda_1 = \lambda_1(\lambda)$ for (3.17) and (3.19) has been found, we may integrate the equation $\mathrm{d}r/\mathrm{d}R = \lambda_1(r/R)$ subjected to the initial condition $r(R_*) = \lambda_0 R_*$ to obtain $r(R)$ in an implicit form:

$$\int_{\lambda_0}^{r/R} \frac{\mathrm{d}\lambda}{\lambda_1(\lambda) - \lambda} = \ln\frac{R}{R_*}, \quad R \geqslant R_*. \tag{3.20}$$

We are now in a position to establish a number of properties concerning the solution of (3.11) including the convergence of the integral in (3.20) at finite R/R_* and the behaviour of the solution as $R/R_* \to \infty$. First, we observe that if a solution satisfying (3.12) exists and $\lambda_1 = \lambda$ holds for some value of R greater than R_*, say $\hat{R}$, then it must hold for all R greater than R_* (Sivaloganathan, 1986). This is because if we were to integrate (3.11) subjected to the initial conditions $r(\hat{R}) = \lambda(\hat{R})\hat{R}$, $r'(\hat{R}) = \lambda(\hat{R})$ then $\lambda_1(R) \equiv \lambda(R) \equiv \lambda(\hat{R}) \forall R > R_*$ should necessarily be the unique solution, since $(3.15)_1$ holds. It then follows from the fact $\lambda_0 \neq \lambda_1^*$ and

$$\frac{\mathrm{d}\lambda}{\mathrm{d}R} = \frac{1}{R}(\lambda_1 - \lambda), \tag{3.21}$$

$$\frac{\mathrm{d}\tau_1}{\mathrm{d}R} = \frac{1}{R\lambda^3}(\lambda \bar{W}_2 - 2\lambda_1 \bar{W}_1) \tag{3.22}$$

(obtained by differentiating $\lambda = r/R$ and $(3.9)_1$, and making use of (3.11)) that the sign of $\mathrm{d}\lambda/\mathrm{d}R$ and $\mathrm{d}\tau_1/\mathrm{d}R$ must be definite for $R \in (R_*, 1]$. This in turn leads to the following properties of equilibrium spherically symmetric two-phase deformations (cf. Sivaloganathan, 1986).

Proposition 3.1. *If $r(R)$ is a solution of (3.11) satisfying (3.12), (3.13) and $(3.15)_1$, then $\lambda(R)$ is a strictly monotone function on $(R_*, 1]$:*

$$\mathrm{d}\lambda/\mathrm{d}R < 0, \ \lambda_1(R) < \lambda(R) \quad \text{if } \lambda_1^* < \lambda_0, \tag{3.23}$$

$$\mathrm{d}\lambda/\mathrm{d}R > 0, \ \lambda_1(R) > \lambda(R) \quad \text{if } \lambda_1^* > \lambda_0. \tag{3.24}$$

If, in addition, (3.15) holds, then the radial Cauchy stress $\tau_1 = \lambda^{-2}\bar{W}_1$ is also a strictly monotone function on $(R_*, 1]$:

$$\mathrm{d}\tau_1/\mathrm{d}R > 0, \quad \textit{if } \lambda_1^* < \lambda_0,$$
$$\mathrm{d}\tau_1/\mathrm{d}R < 0, \quad \textit{if } \lambda_1^* > \lambda_0.$$

If a solution satisfies (3.12), (3.13), $(3.15)_1$ *and* (3.18) *then* $\mathrm{d}\lambda_1/\mathrm{d}\lambda < 0$, $\lambda_1(R)$ *is a strictly monotone function on* $(R_*, 1]$, *and*

$$\mathrm{d}\lambda_1/\mathrm{d}R > 0, \ \lambda_1^* < \lambda_1 < \lambda < \lambda_0 \quad \textit{if } \lambda_1^* < \lambda_0, \tag{3.25}$$
$$\mathrm{d}\lambda_1/\mathrm{d}R < 0, \ \lambda_1^* > \lambda_1 > \lambda > \lambda_0 \quad \textit{if } \lambda_1^* < \lambda_0. \tag{3.26}$$

The proof immediately follows from (3.21), (3.22), $(3.15)_2$, (3.17) and (3.18).

Proposition 3.2. *Let* $r(R)$ *be a solution of* (3.11) *satisfying* (3.12), (3.13). *Let* $(3.15)_1$ *and* (3.18) *hold on a maximal interval* (R_*, R_{max}) *of existence of the solution. Then* R_{max} *is infinite, i.e. r is extendable to* $r \in C^2(R_*, \infty)$ *such that* (3.23), (3.24) *and* (3.25), (3.26) *hold for* $R \in (R_*, \infty)$, *and*

$$\exists \lambda_c : \lim_{R/R_* \to \infty} \lambda = \lim_{R/R_* \to \infty} \lambda_1 = \lambda_c, \tag{3.27}$$
$$\lambda_1^* < \lambda_1 < \lambda_c < \lambda < \lambda_0 \ \textit{or} \ \lambda_1^* > \lambda_1 > \lambda_c > \lambda > \lambda_0 \quad \textit{for } R > R_*. \tag{3.28}$$

Proof. Following Sivaloganathan (1986), we note that by the continuation principle r may be extended to a maximal interval of existence $(R_*, R_{\max})$, $R_{\max} > 1$ such that (3.23), (3.24) and (3.25), (3.26) hold on $(R_*, R_{\max})$ and then show that $R_{\max}$ cannot be finite. If $R_{\max}$ were finite then the following cases could correspond to degenerations of the extended solution (3.12) as $R \to R_{\max} < \infty$: (i) $r(R) \to \infty$, (ii) $r'(R) \to \infty$, (iii) $r(R) \to 0$, (iv) $r'(R) \to 0$. From (3.23), (3.24) it follows that (i) and (ii) are impossible if $\lambda_1^* < \lambda_0$ whereas (iii) and (iv) are impossible if $\lambda_1^* > \lambda_0$.

Now prove impossibility of (iii) and (iv) when $\lambda_1^* < \lambda_0$. By (3.23) and (3.25), $\lambda(R)$ decreases monotonically, whereas $\lambda_1(R)$ increases monotonically as R increases, and $\lambda(R) < \lambda_0$, $\lambda_1(R) > \lambda_1^* > 0$. Then the inequality $\lambda_1(R) - \lambda(R) < 0$ fails at some $\hat{R} \in (R_*, R_{\max})$ if $\lambda(R) \to 0$ as $R \to R_{\max}$. Thus, (iii) is a contradiction if $R_{\max} < \infty$, whereas (iv) contradicts the monotone increasing property of $\lambda_1(R)$. Impossibility of (i) and (ii) when $\lambda_1^* > \lambda_0$ is proved analogously.

From the fact that (3.25), (3.26) hold we then conclude that the integrand in (3.20) is continuous for $\lambda \in [r/R, \lambda_0]$ and the integral converges at any finite R/R_* which corresponds to some value of r/R. By (3.20), $r(R)/R$ is a bounded and monotone function of R/R_*; then

$$\exists \lambda_c \in (\lambda_1^*, \lambda_0) \text{ or } (\lambda_0, \lambda_1^*) : r/R = \lambda(R/R_*) \to \lambda_c \text{ as } R/R_* \to \infty.$$

The limits on the integral in (3.20) are both finite. As $R/R_* \to \infty$, the right hand side of (3.20) tends to infinity and so we must necessarily have $\lambda_1(\lambda) \to \lambda \to \lambda_c$. Finally we obtain (3.28). □

Eq. (3.20) determines a curve on the $(R/R_*, r/R)$-plane (Fig. 2). The curve starts from the point $(1, \lambda_0)$ and, as established above, asymptotically approaches the line $r/R = \lambda_c$ as $R/R_* \to \infty$. The value λ_c corresponds to crossing of the curve $\lambda_1 = \lambda_1(\lambda)$ obtained from (3.17) and (3.19) with the hydrostatic line $\lambda_1 = \lambda$, i.e. $\lambda_1(\lambda_c) = \lambda_c$. Obviously, λ_c is a material parameter as well as λ_0 and λ_1^*. For every pair λ_0, λ_1^* satisfying (3.3) there is a corresponding value of λ_c.

The solutions of (3.11), (3.13) for various R_* correspond to various segments on the single curve (3.20). Segments DD_2, DD_3, DD_4 in Fig. 2a (for the case $\lambda_0 > \lambda_1^*$) and BB_3, BB_2, BB_1 in Fig. 2b (for the case $\lambda_0 < \lambda_1^*$) represent the solutions for three typical values of R_*.

Since the limit $R/R_* \to \infty$ can be obtained by either $R \to \infty$ or $R_* \to 0$, the hydrostatic limiting state $\lambda_1 = \lambda = \lambda_c$ may correspond to either a finite R_* and infinite R (a finite nucleus forming in an infinite medium under an all-round stretching λ_c) or a vanishingly small R_* and finite R (an infinitesimally small new phase forming at the center of a finite sphere).

Note that, on the one hand, $\lambda_1 = \lambda$ identically satisfies (3.11) for all λ but only $\lambda_1 = \lambda = \lambda_c$ is consistent with the initial conditions (3.13). On the other hand, as we move along the hydrostatic axis $\lambda_1 = \lambda$, a phase transformation first becomes possible in the center when $\lambda = \lambda_c$. The topology of solution changes: a uniform

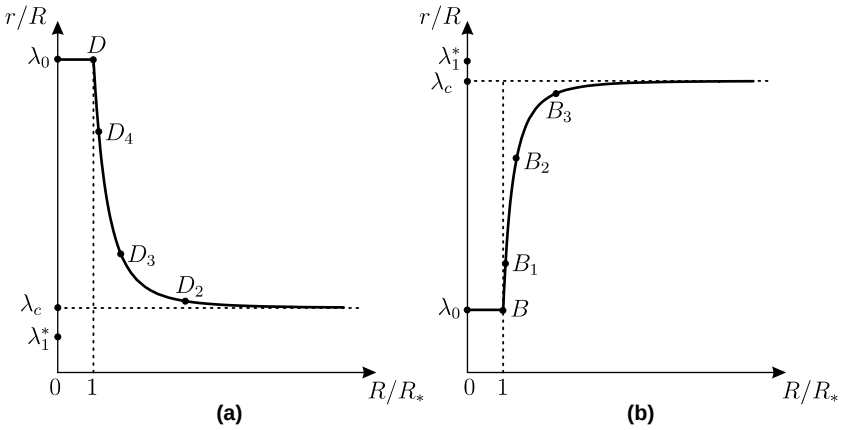

Fig. 2. Equilibrium spherically symmetric two-phase deformations: (a) $\lambda_0 > \lambda_1^*$, (b) $\lambda_0 < \lambda_1^*$.

one-phase state may bifurcate into an equilibrium two-phase state for which one of the phases is localized at the central point.

In the case of a unit sphere the dependence of R_* on $r_0 = r(1)$ is given by

$$R_* = \exp\left\{\int_{\lambda_0}^{r_0} \frac{\mathrm{d}\lambda}{\lambda - \lambda_1(\lambda)}\right\}, \quad R_* \in (0,1). \tag{3.29}$$

By (3.29) and (3.28), the interface radius is a monotone increasing function of r_0 if $\lambda_0 > \lambda_1^*$ or a monotone decreasing function if $\lambda_0 < \lambda_1^*$.

If there are reasons to think that both phases may be localized at the center then one may expect that at least two values of λ_c exist and, thus, at least two pairs of λ_0, λ_1^* and two two-phase equilibrium solutions are possible. One λ_c corresponds to the new phase nucleation in the center. Another λ_c corresponds to the state when the parent phase is localized at the center surrounded by a new phase material. For one of the solutions $\lambda_0 > \lambda_1^*$. For the other one $\lambda_0 < \lambda_1^*$ (see examples in the next subsections).

Further we will see that λ_0 corresponds to the bifurcation of a sphere from a one-phase state into a two-phase state with an infinitesimally thin layer of new phase forming at the outer surface of the sphere.

The above semi-inverse procedure may be used to find the displacement on the boundary in the case of a spherically symmetric two-phase deformation in a body of arbitrary shape. One only needs to integrate (3.11) along the radius from the interface point until the outer boundary point $R = R_0(\Theta, \Phi)$ and compute $r_0 = r(R_0, \Theta, \Phi)$. This includes the case of a sphere where a new spherical phase initiates from a point different from the center. In this case displacements will be different at various points of the outer boundary. Displacements on the boundary $R = R_0(\Theta, \Phi)$ of a possibly non-spherical body and the interface radius are related by

$$R_* = R_0 \exp\left\{\int_{\lambda_0}^{r_0(R_0,\Theta,\Phi)/R_0} \frac{\mathrm{d}\lambda}{\lambda - \lambda_1(\lambda)}\right\}, \quad R_* \in (0, R_0).$$

To conclude this subsection, we note that the solution $\lambda_1 = \lambda_1(\lambda)$ of (3.17), (3.19) is found irrespectively of the relations between λ, λ_1 and r given by (3.6). The curve of the solution $\lambda_1 = \lambda_1(\lambda)$ may cross the line $\lambda_1 = \lambda$ and contain points in which $\lambda_1 > \lambda$ as well as $\lambda_1 < \lambda$, but only those parts of the curve λ_1 against λ which satisfy kinematic compatibility restrictions (3.23), (3.24) may correspond to the solution $r(R)$. Obviously, these parts cannot spread beyond the point $\lambda = \lambda_1 = \lambda_c$.

3.2. The Hadamard material

We now specialize to the Hadamard material for which W takes the form

$$W = \frac{c}{2} I_1 + \frac{d}{2} I_2 + \phi(J), \quad c, d \geqslant 0, \ \ c + d \neq 0. \tag{3.30}$$

Eq. (3.11) then takes the form

$$R\left\{c+2d\left(\frac{r}{R}\right)^2+\ddot{\phi}\left(\frac{r}{R}\right)^4\right\}r''+2\left\{d+\ddot{\phi}\left(\frac{r}{R}\right)^2\right\}\left(\frac{r}{R}\right)r'^2+2\left\{c-\ddot{\phi}\left(\frac{r}{R}\right)^4\right\}r'-\frac{2r}{R}\left\{c+d\left(\frac{r}{R}\right)^2\right\}=0, \tag{3.31}$$

where a dot denotes differentiation with respect to J and use has been made of (3.6).

Two-phase deformations of the Hadamard material has been studied by Freidin and Chiskis (1994a) and Freidin et al. (2002) in the context of PTZ construction and by Fu and Freidin (2004) in the context of stability analysis of piecewise-homogeneous deformations. Here we summarize some of their results and specialize to spherically symmetric deformations.

Since now $[\![W_1]\!]=[\![W_2]\!]=0$, it follows from (2.17) and (2.18) that

$$\mathbf{h}=\mathbf{0},\quad \mathbf{c}=[\![J]\!]\mathbf{n}. \tag{3.32}$$

The traction continuity condition (2.13) and the Maxwell relation (2.14) then take the form

$$cG_1+dG_{-1}=U(J_+,J_-),\quad \frac{\phi_+-\phi_-}{J_+-J_-}=\frac{1}{2}(\dot{\phi}_++\dot{\phi}_-), \tag{3.33}$$

where

$$U(J_+,J_-)\triangleq -\frac{\dot{\phi}_+-\dot{\phi}_-}{J_+-J_-}.$$

For the special problem under consideration $G_1=1/\lambda_0^4$, $G_{-1}=2/\lambda_0^2$, $J_+-J_-=\lambda_0^2(\lambda_1^*-\lambda_0)$, and these two conditions reduce to

$$\frac{c}{\lambda_0^2}+2d=-\frac{\dot{\phi}_+-\dot{\phi}_-}{\lambda_1^*-\lambda_0},\quad \frac{\phi_+-\phi_-}{\lambda_0^2(\lambda_1^*-\lambda_0)}=\frac{1}{2}(\dot{\phi}_++\dot{\phi}_-), \tag{3.34}$$

where $\phi_-=\phi(\lambda_0^3)$, $\phi_+=\phi(\lambda_0^2\lambda_1^*)$. Eqs. $(3.34)_{1,2}$ are two algebraic equations for the two unknown positive constants λ_0 and λ_1^*. The equations, and hence the spherically symmetric problem under consideration, may have a number of solutions. We now show that the number of solutions and other qualitative features can be deduced a priori with the aid of the corresponding PTZ.

Following Freidin and Chiskis (1994a), we may first solve $(3.33)_2$ to obtain $J_+=J_+(J_-)$. Then $(3.33)_1$ reduces to

$$cG_1+dG_{-1}=u(J_-),\quad \text{where } u(J_-)\triangleq U(J_+(J_-),J_-). \tag{3.35}$$

The PTZ in the space of principal stretches is then formed by all those triads of stretches for which the straight line given by (3.35) intersects the triangular region in Fig. 1. Clearly, cG_1+dG_{-1} attains its minimum and maximum at the vertexes of the triangle $\mathscr{G}$. If $\lambda_1<\lambda_2<\lambda_3$ then

$$\min_{G_1,G_{-1}\subset\mathscr{G}}(cG_1+dG_{-1})=h(\lambda_2,\lambda_3),\quad \mathbf{n}=\mathbf{e}_1,$$
$$\max_{G_1,G_{-1}\subset\mathscr{G}}(cG_1+dG_{-1})=h(\lambda_2,\lambda_1),\quad \mathbf{n}=\mathbf{e}_3,$$

where

$$h(\lambda_i,\lambda_j)=\frac{c}{\lambda_i^2\lambda_j^2}+d\left(\frac{1}{\lambda_i^2}+\frac{1}{\lambda_j^2}\right).$$

Thus, the PTZ is bounded by the two surfaces $u(J)=h(\lambda_2,\lambda_3)$ and $u(J)=h(\lambda_2,\lambda_1)$. For the present problem where $\lambda_2=\lambda_3\equiv\lambda$, the two surfaces reduce to two curves on the (λ_1,λ)-plane:

$$u(J)=h(\lambda,\lambda),\ \text{corresponding to } \mathbf{n}=\mathbf{e}_1 \tag{3.36}$$

and

$$u(J)=h(\lambda,\lambda_1),\ \text{corresponding to } \mathbf{n}\perp\mathbf{e}_1. \tag{3.37}$$

The strong ellipticity conditions for the material (3.30) reduce to

$$h(\lambda_{\mathrm{mid}}, \lambda_{\max}) + \ddot{\phi} > 0 \tag{3.38}$$

where λ_{mid} and $\lambda_{\max}$ are intermediate and maximal stretches, respectively, see Rosakis (1990), Freidin and Chiskis (1994a). Then with $\lambda_2 = \lambda_3 \equiv \lambda$ a non-ellipticity sub-zone is described by

$$h(\lambda, \lambda_1) + \ddot{\phi} < 0 \quad \text{if } \lambda < \lambda_1, \tag{3.39}$$

$$h(\lambda, \lambda) + \ddot{\phi} < 0 \quad \text{if } \lambda > \lambda_1. \tag{3.40}$$

We choose the function Φ such that the non-ellipticity sub-zone is embedded in the PTZ. Note that from (3.38) and

$$\frac{\tilde{W}_1 - \tilde{W}_2}{\lambda_1 - \lambda_2} + \tilde{W}_{12} = c + d(\lambda_1\lambda_2 + \lambda_3^2) + \lambda_1\lambda_2\lambda_3^2\ddot{\phi}$$

it follows that if the Hadamard material is strongly elliptic at λ_1, λ_2, λ_3 then the assumption (3.18) holds.

To proceed further, we now assume that $\phi(J)$ takes the simple form (Freidin and Chiskis, 1994a)

$$\phi(J) = \frac{(J - J_c)^4}{4} - \frac{A(J - J_c)^2}{2} + a(J - J_c), \tag{3.41}$$

which gives $u(J) = A - (J - J_c)^2$, where J_c, A and a are material constants. We note that this model does not satisfy the condition $W \to \infty$ as $J \to 0$, and so it should be applied with caution when very small principal stretches are involved.

The PTZ and the non-ellipticity sub-zone for the Hadamard material with ϕ given by (3.41) at $\lambda_2 = \lambda_3 \equiv \lambda$ is shown in Fig. 3. The thin dotted line corresponds to $J = J_c$. The hashed area denotes the non-ellipticity sub-zone, and the shaded area represents the interior of the PTZ. The material parameters are chosen such that (i) the material is strongly elliptic at the interface, (ii) the stress-free state $\lambda_1 = \lambda_2 = \lambda_3 = 1$ is outside the PTZ, and (iii) stress is zero and the bulk modulus is positive at $\lambda_1 = \lambda_2 = \lambda_3 = 1$.

The thick solid line in the main figure denotes the PTZ boundary corresponding to $\mathbf{n} = \mathbf{e}_1$ and is given by Eq. (3.36). Only λ_1 may suffer a jump if the PTZ is reached for example at point M or N.

The thick dotted line denotes the PTZ boundary corresponding to the normal $\mathbf{n} \perp \mathbf{e}_1$. If $\mathbf{B}_- = \lambda_1^2\mathbf{e}_1 \otimes \mathbf{e}_1 + \lambda^2(\mathbf{I} - \mathbf{e}_1 \otimes \mathbf{e}_1)$ and $\mathbf{n} \perp \mathbf{e}_1$ then the eigenvectors of $\mathbf{B}_+$ can be ordered such that

$$\mathbf{B}_+ = \lambda_1^2\mathbf{e}_1 \otimes \mathbf{e}_1 + \lambda^2\mathbf{e}_2^+ \otimes \mathbf{e}_2^+ + \lambda_{3+}^2\mathbf{e}_3^+ \otimes \mathbf{e}_3^+, \quad \mathbf{e}_3^+ = \mathbf{n}, \quad \mathbf{e}_2^+ = \mathbf{e}_1 \wedge \mathbf{n}.$$

Thus, $\mathbf{B}_+$ is no longer axially symmetric and cannot be presented on the $\lambda\lambda_1$-plane.

It is seen that either point A or point E may correspond to the spherical deformation in the core phase of the sphere. Thus two solutions of the form (3.1) and (3.2) are possible. One solution is given by $\lambda_0 = \lambda^E$, $\lambda_1^* = \lambda_1^D$, and the other is given by $\lambda_0 = \lambda^A$, $\lambda_1^* = \lambda_1^B$. The arrows AB and ED denote the corresponding jumps in λ_1.

The first solution (namely $\lambda_0 = \lambda^E$, $\lambda_1^* = \lambda_1^D$) corresponds to a spherical nucleus of new phase forming from the center. The point E represents the spherical deformation inside the nucleus. Such a phase transformation first takes place in the center under all-round stretching from the undeformed state when point D_1 is reached. As discussed above, the point D_1 also corresponds to an all-round stretching $\lambda_c^{D_1}$ at which a finite spherical nucleus of a new phase may appear in an infinite medium. As soon as the new phase with a vanishingly small radius first appears, the deformation in the initial phase changes discontinuously from being spherical to being spherically symmetric. The deformation on the initial-phase side of the interface is represented by D. The line segment DD_1 shows the distribution of (λ, λ_1) in the outer shell "made" of the initial phase at the moment of the new phase nucleation.

The radius of the nucleus increases as r_0 increases (Fig. 4a). The deformations on the interface remain to be the same constants represented by the points E and D. Deformations in the outer shell change in a such way that the point corresponding to the deformation at $R = 1$ moves towards point D along DD_1. For example, at some intermediate value of r_0 the distribution of (λ, λ_1) in the outer phase is represented by the segment DD_2. At another moment the distribution corresponds to the segment DD_3. The transformation finishes at

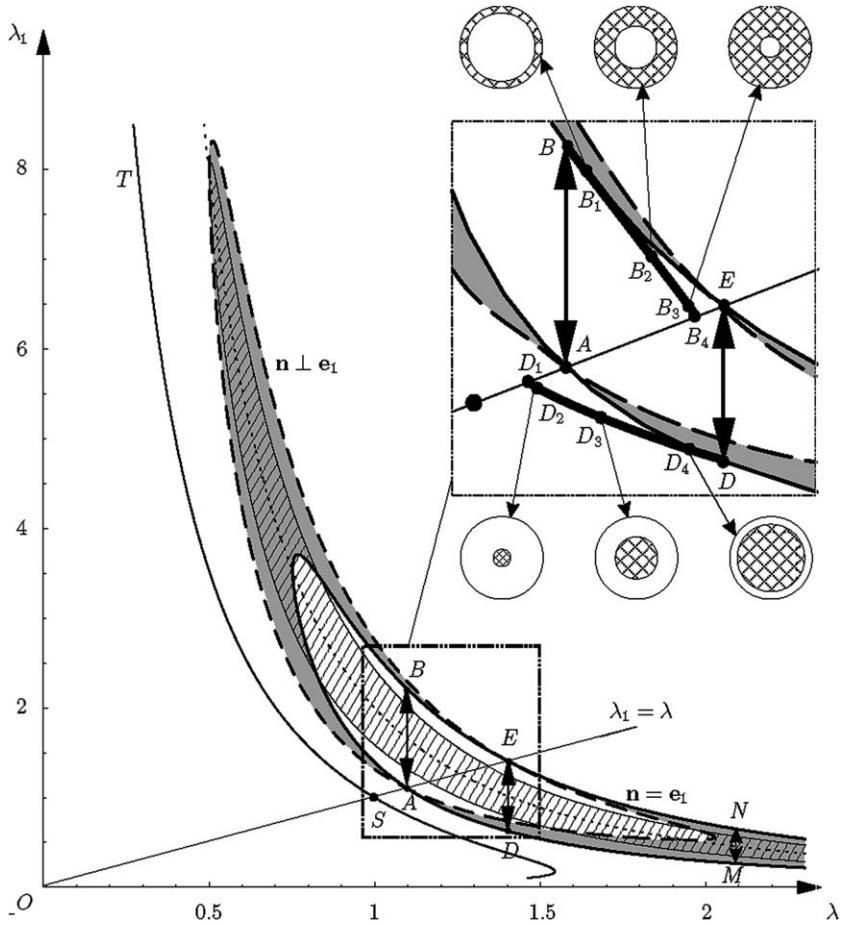

Fig. 3. The PTZ on the $\lambda\lambda_1$-plane for the Hadamard material with $J_c = 2$, $d = 0.2$, $A = 0.8$, $c = 0.03$, $a = -0.23$. ST: path of uniaxial stretching; EDD_1 and ABB_4: spherically symmetric deformations.

$r_0 = r_0^E = \lambda^E$ when the deformation is again spherical. The corresponding solutions on the $(R/R_*, r/R)$-plane are pictured in Fig. 2a.

In the unloading process from the new phase state we start from point E. A thin spherical layer of the initial phase appears and spread into the interior of the sphere as r_0 decreases.

We emphasize that in this scenario deformations throughout the sphere are *outside* or on the external PTZ boundary.

Note one more feature of the equilibrium two-phase deformation. In the case of small strains the volume strain presented by the first invariant of the linear strain tensor is piecewise constant if the deformation is spherically symmetric, and the constants only depend on material parameters (see Morozov et al., 1996; Nazyrov and Freidin, 1998). In Fig. 5 we have shown how J is distributed in the present case. One can observe the tendency to piecewise-constant distribution of J, and the character does not depend on R_*. One constant is always equal to $J_E = (\lambda^E)^3$ and represents the internal phase. The values of J in the outer phase varies between two fixed values $J_D = (\lambda^E)^2\lambda_1^E$ and $J_{D_1} = (\lambda_c^{D_1})^3$ for all R_*. The value J_{D_1} would be the asymptotic value of J if we were to integrate (3.11) subject to (3.13) beyond $R = R_*$ to infinity (see the dashed lines in Fig. 5b). In this case DD_1 can be viewed as showing the strain distribution in $R \in (R_*, \infty)$ in an equilibrium two-phase infinite medium subjected to an all-round stretching $\lambda_c^{D_1}$.

As a comparison, we have used dashed lines in Fig. 5a to demonstrate the distribution of J when the interface radius is slightly perturbed from $R_* = 0.7$ with r_0 held fixed. The perturbed solutions satisfy all the equilibrium conditions except the Maxwell relation (to be more precise, the perturbation solution is obtained by

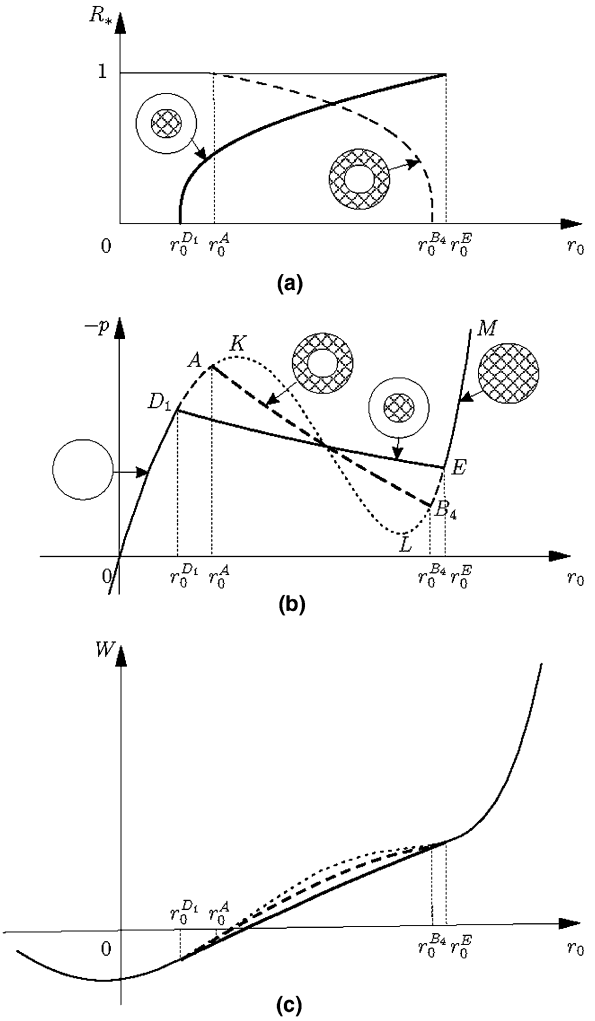

Fig. 4. Two types of two-phase solutions compared with the single-phase solution for the Hadamard material. Solid lines: the first two-phase solution. Dashed lines: the second two-phase solution. Dotted lines: the one-phase solution.

integrating (3.31) subjected again to the initial conditions (3.13) but now λ_1^*, λ_0 are determined by $r(1) = r_0$ and the traction continuity condition). It is seen that the solutions that do not satisfy the Maxwell relation vary more significantly.

The distribution of J represents the volume part of the deformation. For completeness' sake we also show in Fig. 6 distributions of $\lambda_\Phi - \lambda_R$ which characterize deviations from a spherical strain state. This quantity is equal to *zero* in the internal phase. Its distributions in the outer shell are similar for various equilibrium interfaces (Fig. 6a) and may be much more different if the interface radius does not satisfy the Maxwell relation (see Fig. 6b where the solid line corresponds to the equilibrium two-phase deformation and dashed lines correspond to perturbed interface radii at the same r_0).

We now turn to the second solution corresponding to $\lambda_0 = \lambda^A$, $\lambda_1^* = \lambda_1^B$. In this case the interface begins to spread from the outer surface when $r_0 = r_0^A = \lambda^A$ (Fig. 4a). A thin spherical layer appears with the deformation corresponding to point B in Fig. 3. The sphere completely transforms into the new phase when $r_0 = \lambda_c^{B_4}$. Deformations in the new phase correspond to the parts of the segment BB_4 in Fig. 3 such as BB_2 as the interface moves towards the center of the sphere. See also Fig. 2b. At the last moment just before the transformation is finished the deformations in the body are given by the point A (for the origin) and the segment BB_4 (for the rest of the sphere). As soon as the material at the center is transformed into the new phase, the deformation

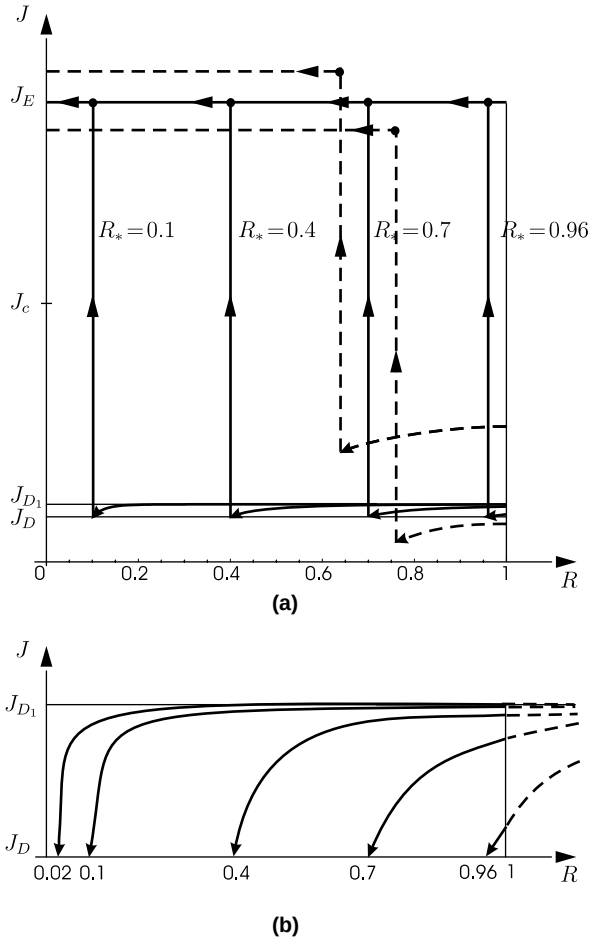

Fig. 5. Variations of J for various R_*: (a) in the whole sphere; (b) in the outer layer (the dashed lines show the asymptotic behaviour if integration of (3.31) is carried out beyond $R = 1$).

in the whole sphere becomes uniform again and corresponds to the single point B_4. We note that in this scenario point B belongs to the internal PTZ boundary and deformations in some part of the sphere correspond to points inside the internal boundary of the PTZ. The values of J inside the shell remain between $J_B = (\lambda_0^A)^2\lambda_1^B$ and $J_{B_4} = (\lambda_c^{B_4})^3$.

Note the following similarity and difference between points D_1 and B_4. Both D_1 and B_4 are bifurcation points at which a uniform spherical deformation may bifurcate into a corresponding two-phase deformation. The first two-phase solution exists for $r_0^{D_1} < r_0 < r_0^E$, whereas the second two-phase solution only exists for $r_0^A < r_0 < r_0^{B_4}$ (see Fig. 3). Thus, in the vicinity of point D_1 with $\lambda_c^{D_1} < r_0 = \lambda_1 = \lambda < r_0^A$ there are no other two-phase spherically-symmetric deformations than the one given by the first solution. In the vicinity of B_4 with $r_0 < \lambda_c^{B_4}$ we have both two-phase solutions.

The dependence of the required pressure $p = -\tau_1|_{R=1}$ on the external radius r_0 is shown in Fig. 4b. If the sphere were deformed uniformly we would have the diagram $0KLM$. Thick solid and dashed lines correspond to the first and second two-phase solutions, respectively. Both solutions demonstrate stress-softening effect on the loading path.

To decide which solution is robust and is most likely to be observed, we now analyze the energy and stability associated with the three solutions. Simple numerical calculations show that, given r_0, both two-phase deformations are energetically preferable to the one-phase deformation (Fig. 4c). If the pressure is prescribed then it can be shown that the potential energy of one of the two one-phase homogeneous states is less than the energy of the corresponding two-phase deformations.

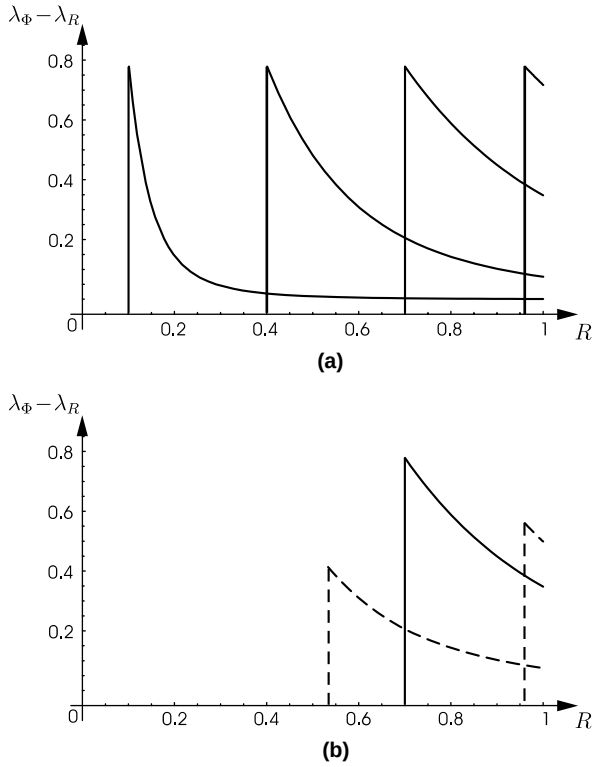

Fig. 6. Variation of $\lambda_\Phi - \lambda_R$ in the sphere: (a) equilibrium two-phase deformations at various r_0; (b) equilibrium (solid) and non-equilibrium (dashed) two-phase deformations at the same $r_0 = 1.21$ ($R_* = 0.7$).

For both two-phase solutions the energy increases if the interface is perturbed in the vicinity of R_* at a given r_0, as shown in Fig. 7 for the first solution. In computing the energy for each perturbed interface the perturbed deformation field is required to satisfy all the equilibrium and jump conditions except the Maxwell relation. It is seen that both solutions are stable with respect to spherical perturbations of the interface. In Section 4 we will show that the second solution is in fact unstable with respect to small wavelength perturbations and, thus, the bifurcation at point B_4 cannot be observed.

We have so far considered two-phase deformations with only one interface. We now show with the aid of the PTZ that no more interfaces are possible. Indeed, (3.31) was integrated subject to initial conditions at $R = R_*$ where the deformation is represented by points D or B in Fig. 3. The segment DD_1 corresponds to the first solution when the new phase first appears. If another spherical interface at $R_{**} > R_*$ were assumed,

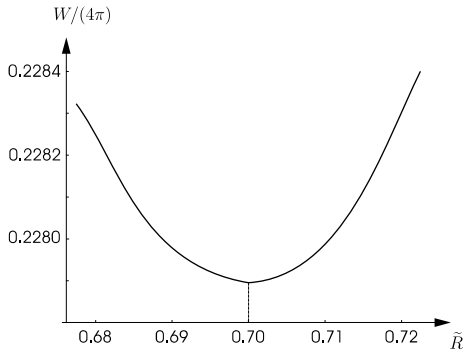

Fig. 7. Dependence of the total energy on the interface radius $\tilde{R}$ when r_0 is fixed; $r_0 = 1.21$, the minimum W is attained at $\tilde{R} = R_* = 0.7$.

deformations for $R \in [R_*, R_{**}]$ would belong to the same line. We would have two spherically symmetric (non-spherical) deformations which could coexist across the second interface. On the other hand, the deformation on any interface must belong to the PTZ by definition. But the DD_1 has only one common point D with the PTZ. Thus, another equilibrium interface is not possible. The same argument can be applied to the second solution. We remark, however, that if the solid sphere is replaced by a hollow sphere, then more than one interface may be possible; see Eremeyev et al. (2002, 2003, in press) for an analysis in the small-strain approach.

To illustrate the point that a phase transformation may not take place even if the dependence of the all-round pressure on the stretch has the usual non-convex form (that is a maximum followed by a minimum), we have shown in Fig. 8 the PTZ cross-section by the plane $\lambda_2 = \lambda_3$ and the dependence of the all-round tension on λ for another set of material parameters. One can conclude directly from an inspection of the PTZ that this material does not allow spherically symmetric phase transformations since the PTZ does not contain a

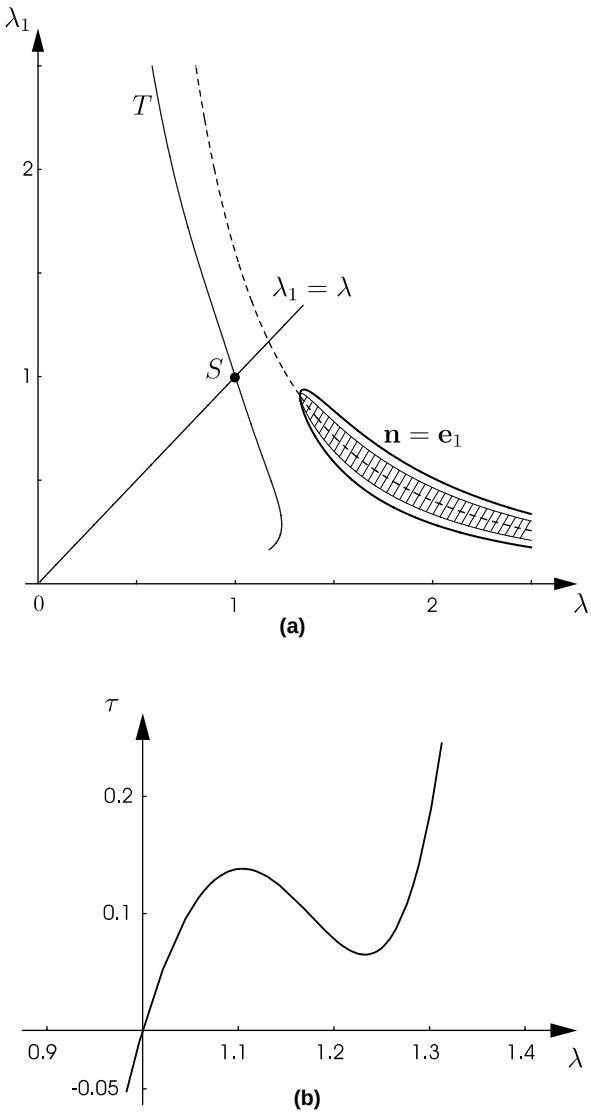

Fig. 8. The PTZ on the $\lambda_1\lambda$-plane (a), and the dependence of the Cauchy hydrostatic stress τ on the all-rounding stretching λ (b) for the Hadamard material with $J_c = 1.6$, $d = 0.3$, $A = 0.35$, $c = 0.03$, $a = -0.624$.

point at which $\lambda_1 = \lambda$. But the corresponding strain energy is a non-convex function of λ. This curve, as well as the tension-stretch curve, looks very similar to that corresponding to Fig. 4.

To conclude this section we note that not every loading path will lead to a phase transformation. We demonstrate this by considering piecewise-homogeneous two-phase deformations. Since the PTZ is constructed from an analysis of local equilibrium conditions, every point of the PTZ corresponds to a piecewise-homogeneous two-phase deformation. One can see that the line ST in Fig. 3 showing the deformation path of a uniaxial stretching does not intersect the PTZ. This means that piecewise-homogeneous two-phase deformations cannot appear under uniaxial stretching.

3.3. A model material with W depending on I_1 and J

Phase transformations in the Hadamard material are possible if the function $\phi(J)$ satisfies certain conditions. The loss of ellipticity at some deformation gradients is one of the conditions. In this section we consider the following material model proposed by Freidin and Chiskis (1994a) and used in the PTZ construction by Freidin et al. (2002) and Freidin and Vilchevskaya (2002):

$$W(I_1, J) = V(I_1) + \Phi(J), \tag{3.42}$$

$$V(I_1) = \begin{cases} c_1 I_1, & I_1 \in (0, I_c), \\ c_2(I_1 - I_c) + c_1 I_c, & I_1 \in (I_c, \infty), \end{cases} \quad c_1 > c_2, \tag{3.43}$$

$$\Phi(J) = aJ^2 + bJ + c, \tag{3.44}$$

where c_1, c_2, I_c, a, b, c are material constants. The constants b and c are expressed in terms of the others such that the strain energy and stresses vanish at the undeformed state. Other restrictions follow from an examination of ellipticity. We take $I_c > 3$. Then it can be shown that the strong ellipticity condition is satisfied at the undeformed state if $a > c_1/3$, and that the Poisson's ratio is positive at the undeformed state if $a > c_1$. The strain-energy function admits two-phase deformations due to its special dependence on the first strain invariant. The non-ellipticity area degenerates to a surface $I = I_c$ in the strain space.

Note that the strain-energy function only depends on the first and third strain invariants. As observed in Freidin and Chiskis (1994a), in this case it follows from (2.17) and (2.18) that

$$\mathbf{h} = -\frac{[W_1]}{W_1^+ G_1}\mathbf{t}_1^-. \tag{3.45}$$

Substituting (3.45) into (2.10) gives (see Freidin et al., 2002)

$$[I_1] = G_1[J^2] - \frac{[W_1^2]}{W_{1+}^2} L_1^-, \tag{3.46}$$

$$L_1 \triangleq G_1^{-1}\mathbf{t}_1 \cdot \mathbf{t}_1 = I_1 - J^2 G_1 - G_{-1}G_1^{-1}. \tag{3.47}$$

The traction continuity condition (2.13) and the Maxwell relation (2.14) then reduce to

$$2G_1[JW_1] = -[W_3], \tag{3.48}$$

$$[W] = \frac{W_1^- W_3^+ + W_1^+ W_3^-}{W_1^- + W_1^+}[J] + \frac{2W_1^- W_1^+}{W_1^- + W_1^+}[I_1]. \tag{3.49}$$

The three equations (3.46), (3.48) and (3.49) contain the four unknowns J_+, I_1^+, G_1 and G_{-1}. If we solve (3.48) and (3.49) to obtain

$$J_+ = J_+(G_1, J_-, I_1^-), \quad I_1^+ = I_1^+(G_1^-, J_-, I_1^-), \tag{3.50}$$

and then substitute (3.50) into (3.46), we obtain an equation which is linear in G_{-1}:

$$\Psi \triangleq \Psi_1(G_1, J, I_1) + \Psi_2(G_1, J, I_1)G_{-1} = 0, \tag{3.51}$$

where we have removed the superscripts/subscripts "−" since (3.51) is also valid for the "+" phase.

Eq. (3.51) determines a curve on the $(G_1,\ G_{-1})$-plane. Its intersection with the triangular region $\mathscr{G}$ in Fig. 1 yields a one-parameter family of orientation invariants. The corresponding values of I_1^+ and J_+ are calculated from (3.50).

Since the function Ψ is linear in G_{-1}, its maximal and minimal values are reached, given λ_i, on the boundary of $\mathscr{G}$. If $\lambda_1 < \lambda_2 < \lambda_3$, then one of these values is reached on the A_1A_3-side of the triangle $\mathscr{G}$. The corresponding normal lies in the (1,3)-principal plane of $\mathbf{B}$.

For the specific material model (3.42)–(3.44) the conditions (3.46)–(3.49) reduce to the system of equations:

$$[I_1] = (J_+^2 - J_-^2)G_1 + (k^2-1)L_1, \tag{3.52}$$

$$-A(J_+ - J_-) = (J_+ - kJ_-)G_1, \tag{3.53}$$

$$[I_1] = (k+1)(I_c - I_1^-) - A(J_+ - J_-)^2, \tag{3.54}$$

where

$$A = a/c_2, \quad k = c_1/c_2.$$

Solving (3.53) for J_+ and substituting the resulting expression into (3.52) and (3.54), we obtain a single equation for G_1 and G_{-1}:

$$\frac{J_-^2 G_1^2}{A+G_1} + L_1^- = \frac{I_c - I_1^-}{k-1}. \tag{3.55}$$

The PTZ is determined by the inequalities

$$\min_{G_1,G_{-1}\in\mathscr{G}} \frac{J^2G_1^2}{A+G_1} + L_1 \leqslant \frac{I_c - I_1}{k-1} \leqslant \max_{G_1,G_{-1}\in\mathscr{G}} \frac{J^2G_1^2}{A+G_1} + L_1, \tag{3.56}$$

which apply to both "−" and "+" phases.

On the one hand, if $W \equiv V$, and $J \equiv 1$, then (3.43) describes the incompressible Treloar material that has been considered by Freidin and Chiskis (1994b) as the simplest incompressible material model that allows two-phase deformations (Fig. 9). The "kink" point $I = I_c$ replaces the non-ellipticity sub-zone. For such a material the interface, corresponding to the PTZ boundary, must necessarily be given by $n_1^2 = \lambda_1/(\lambda_1+\lambda_3)$, $n_2 = 0$, $n_3^2 = 1 - n_1^2$ (assuming $\lambda_1 > \lambda_2 > \lambda_3$) and across the interface a shear strain suffers a jump.

On the other hand, the material (3.42) and (3.43) can be considered as a composition of two Hadamard materials which are identified with different phase states of a single material. However, in contrast to the Hadamard material considered in the previous subsection, in the current model it is not the $\Phi(J)$ that gives rise to phase transformations. It can be deduced from (3.56) that two types of interfaces are possible under the present model (Freidin et al., 2002). In the first case, the normal coincides with the eigenvector of $\mathbf{B}^-$ corresponding to *the maximal* stretch, contrary to the Hadamard material in which the normal corresponds to the *minimal* stretch, and only this stretch suffers a jump. In the other case, the interface is similar to the interface in the incompressible Treloar material except that the jump is no longer volume-preserving. We refer to these two types of interfaces as the stretching-type and shearing-type, respectively.

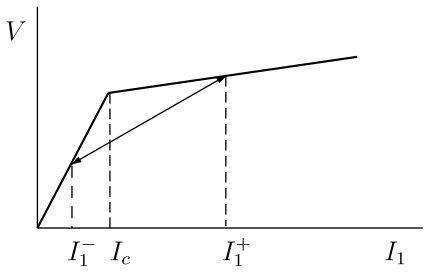

Fig. 9. The kinked function $V(I_1)$ for the model material.

Figs. 10 and 11 show the axially symmetric PTZ cross-sections (by the plane $\lambda_2 = \lambda_3 = \lambda$) and the PTZ cross-section by the plane $\lambda_2 = 1$, respectively. The shaded area represents the interior of the PTZ. We have divided the PTZ boundaries into thick and thin line segments: the thick line segments give rise to shearing-type interfaces, whereas the thin line segments correspond to stretching-type interfaces. The dashed lines denote the internal PTZ boundaries and the dotted lines denote the non-ellipticity surface $I = I_c$. The lines OM and PN correspond to the path of uniaxial tension in the 1-direction

$$\lambda_2 = \lambda_3 = \Lambda(\lambda_1), \quad \tau_2 = \tau_3 = 0 \tag{3.57}$$

(Fig. 10) or "plane" stretching

$$\lambda_2 \equiv 1, \quad \lambda_3 = \Lambda(\lambda_1), \quad \tau_3 = 0 \tag{3.58}$$

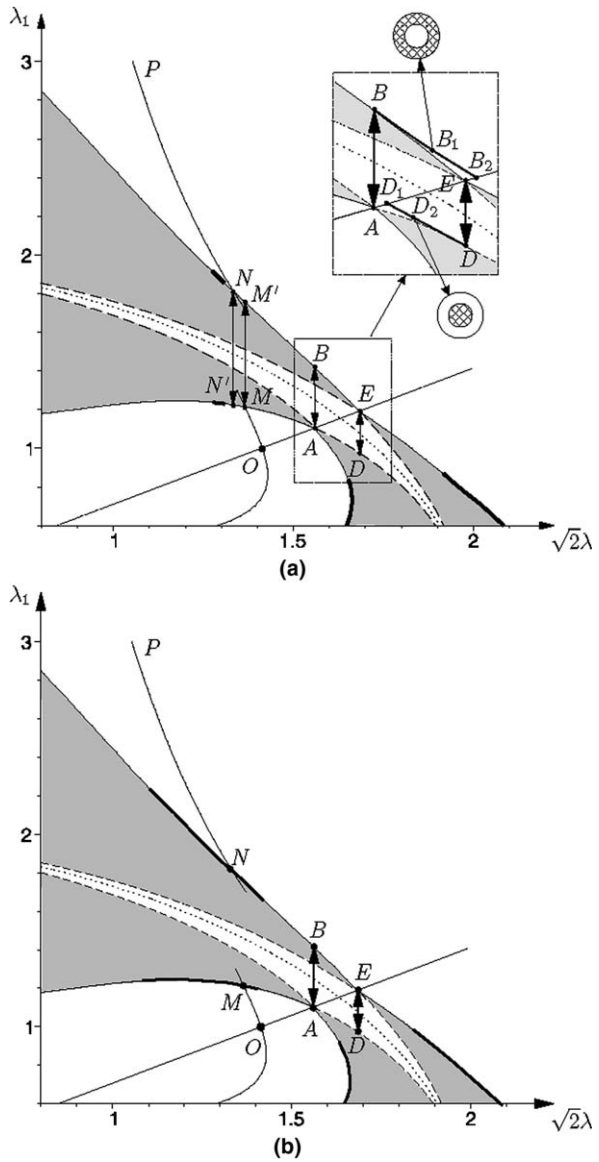

Fig. 10. Axially symmetric PTZ cross-section for the model material. (a) $a = 4.09$, $c_1 = 3$, $c_2 = 1$, $I_c = 4$; (b) $a = 4.4$, $c_1 = 3$, $c_2 = 1$, $I_c = 4$. The lines OM and NP correspond to the path of uniaxial stretching, and the points A, B, D, E refer to spherically symmetric deformations.

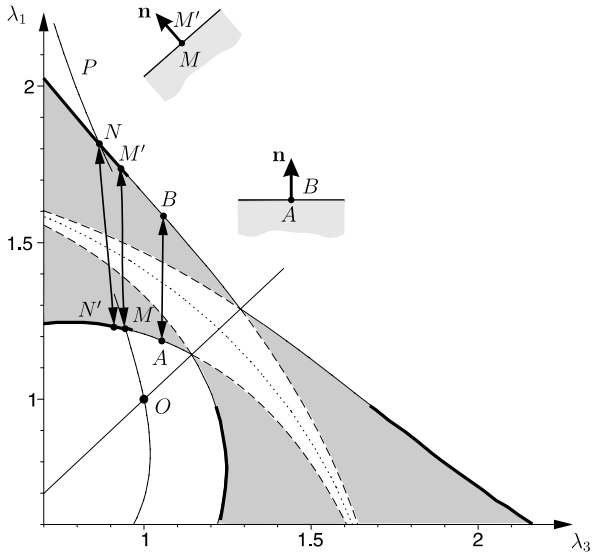

Fig. 11. The PTZ plane section for the model material with $\lambda_2 = 1$, $a = 4.09$, $c_1 = 3$, $c_2 = 1$.

(Fig. 11). It is seen that, depending on material parameters, the crossing points M and N may correspond to either type of interfaces. Even for the same parameters the type of interfaces may be different for uniaxial and plane stretching, and for plane stretching and other plane deformations. For instance, the point M in Fig. 10b corresponds to a shearing-type interface and the jump in strains is directed out of the $\lambda\lambda_1$-plane. On the other hand, point M in Fig. 10a corresponds to the normal $\mathbf{n} = \mathbf{e}_1$, and in this case the jump is represented by MM'.

Note that in Figs. 10a and 11 the point N which denotes crossing of the unloading path with the PTZ does not coincide with point M' where the deformation jumps from the point M. Analogously, the points M and N' are also different. The explanation is that the lines OM and PN satisfy the conditions (3.57) or (3.58). These conditions are satisfied at points M and N, but may be violated at points M' and N' because of stresses induced *by* phase transformations. We do not discuss here how the whole material transforms from the branch OM to the branch PN.

Thus, this model material demonstrates a variety of interfaces for different loading paths. Now we study its behaviour under all-round stretching.

One can see from Fig. 10 that two spherically symmetric solutions are possible. The jumps in strains are represented by AB (the first solution) and ED (the second solution). Using the same procedures as in the case of the Hadamard material one can find the dependence of the equilibrium interface radius on the outer radius of the sphere, construct the pressure-outer radius relation, examine the energies, and relate the two-phase deformations to the PTZ. The results are presented in Fig. 12. A thin spherical layer of a new phase can appear at the outer surface of the sphere when the loading reaches point A. Then the core phase remains to be in a spherical strain state with $\lambda_1 = \lambda_2 = \lambda_3 = \lambda_0^A$. The strains in the outer phase are distributed along BB_1 at some intermediate radius of the interface. The transformation finishes at $r_0 = \lambda_c^{B_2}$.

The second solution corresponds to the nucleation of a new phase from the center of the sphere when $r_0 = \lambda_c^{D_1}$. Strains are distributed as EDD_1, EDD_2, etc.

Both solutions are energetically preferable to the one-phase solution, are stable with respect to radial perturbation of the interface, and displays strain-softening behaviour.

As in the case of the Hadamard material, we refer to the two-phase solution with lower energy as the first solution. We note that parameters c_1, c_2 can be related to the shear modulus of the two phases and that for the first solution the greater c_1 is associated with the core phase. For the chosen material parameters, contrary to the Hadamard material, the first solution corresponds to the nucleation of a new phase from the outer surface of the sphere. Similar to the Hadamard material, strains throughout the sphere are *outside* the PTZ in the case of the first solution and at least some of the strains are inside the external PTZ boundary for the second

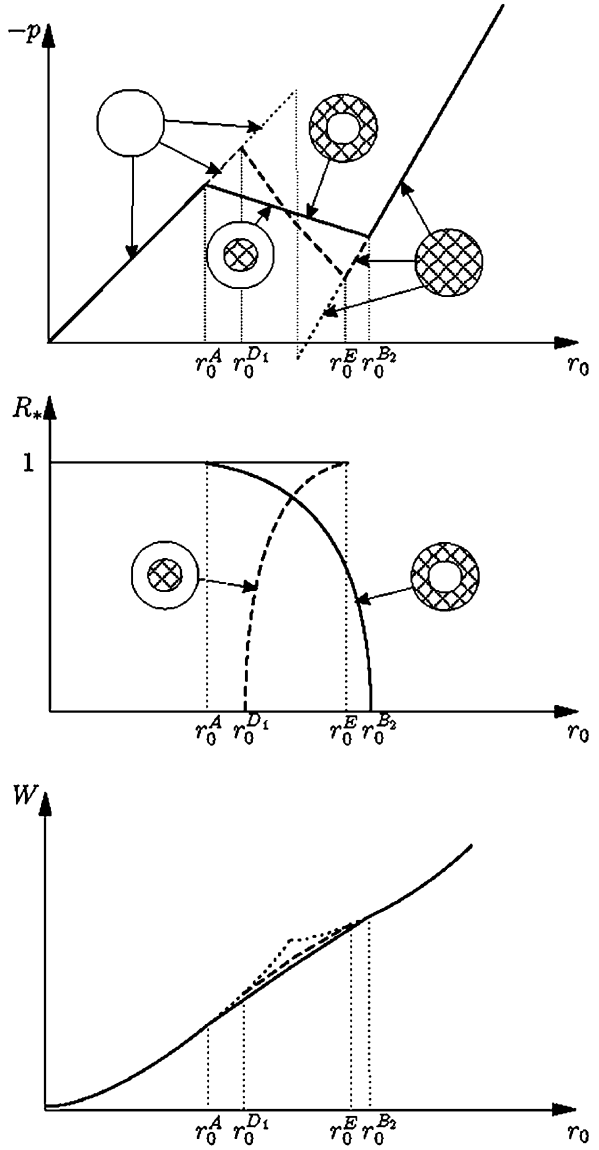

Fig. 12. Two-phase solutions compared with the one-phase solution for the model material.

solution. In the next section it is shown that as in the case of a Hadamard material the second solution is unstable with respect to small wavelength perturbations.

4. Further stability considerations

In the previous section we have considered the stability of the two-phase deformations with respect to spherical perturbations of the interface in the undeformed configuration. In this section, we consider stability with respect to certain small-wavelength perturbations and check whether a necessary stability condition is satisfied or not for the solutions obtained.

It is known (Gurtin, 1983) that if a two-phase inhomogeneous deformation is a local energy minimizer, then given any point $\mathbf{p}_0$ of the interface, the piecewise-homogeneous deformation corresponding to the two values $\mathbf{F}_{\pm}(\mathbf{p}_0)$ is also an energy minimizer. Thus, instability of the latter state would imply instability of the former state.

For the present problem, the pairwise-homogeneous deformation field corresponding to $\mathbf{F}_{\pm}(\mathbf{p}_0)$ is given by

$$\mathbf{F} = \begin{cases} \mathbf{F}_- = \operatorname{diag}\{\lambda_0, \lambda_0, \lambda_0\}, & \text{for } 0 < \mathbf{e}_1 \cdot \mathbf{X} < \infty, \\ \mathbf{F}_+ = \operatorname{diag}\{\lambda_1^*, \lambda_0, \lambda_0\}, & \text{for } -\infty < \mathbf{e}_1 \cdot \mathbf{X} < 0. \end{cases} \tag{4.1}$$

From our discussions in the two previous sections, there are two sets of solutions for λ_0 and λ_1^* for each material model. According to Fu and Freidin (2004), the stability of such a pairwise-homogeneous deformation, with respect to perturbations that are sinusoidal in the $\mathbf{e}_2$-direction and localized near the interface, is determined by the signs of the eigenvalues of the Hermitian matrix H defined by

$$H = \begin{pmatrix} P & \mathbf{g} \\ \hat{\mathbf{g}}^{\mathrm{T}} & \bar{\mathbf{f}} \cdot M^{-}\bar{\mathbf{f}} \end{pmatrix}, \tag{4.2}$$

where

$$P = \hat{M}^{+} + M^{-}, \tag{4.3}$$

$$\mathbf{g} = M^{-}\bar{\mathbf{f}} - \mathrm{i}\boldsymbol{\beta}, \quad \bar{\mathbf{f}} = [\![\mathbf{F}]\!]\mathbf{e}_1, \quad \boldsymbol{\beta} = [\![J\mathbf{T}\mathbf{F}^{-\mathrm{T}}]\!]\mathbf{e}_2. \tag{4.4}$$

In the above expressions, M^{+} and M^{-} are the surface impedance matrices associated with $\mathbf{F}_{+}$ and $\mathbf{F}_{-}$, respectively, and a hat on M^{+} signifies complex conjugation. Explicit formulae for M^{+} and M^{-} are given in Fu and Freidin (2004) and Fu and Brookes (in press) in terms of the elastic moduli.

The pairwise-homogeneous deformation is unstable if at least one of the eigenvalues of H is negative, and is stable if all the eigenvalues of H are positive. The P defined by (4.3) is referred to as the interfacial impedance tensor. Its positive definiteness assures stability of the corresponding joint-problem (that is the problem when the interface in the reference configuration is fixed and is not allowed to vary). It is seen that the positive definiteness of P is a necessary condition for H to be positive definite. Assuming that P is positive definite, Fu and Freidin (2004) showed that H is positive definite if and only if

$$L \triangleq \bar{\mathbf{f}} \cdot M^{-}\bar{\mathbf{f}} - \hat{\mathbf{g}} \cdot P^{-1}\mathbf{g} > 0, \tag{4.5}$$

which is a stability criterion based on kinetic considerations (Eremeyev et al., 2002, 2003). This criterion has the following physical interpretation. If (4.5) is satisfied, energy will be dissipated as the interface is perturbed and the perturbation will eventually die out. If, on the other hand, (4.5) is violated, energy will actually be created as the interface is perturbed, which would lead to further growth of the interface.

Our numerical calculations according to the above recipe show that for both materials the second solution, in which part of the deformations are inside the external PTZ boundaries, is unstable, whereas instability of the other solution, in which the deformations throughout the sphere except those at the interface are outside of the PTZ, is not observed.

5. Conclusions

In the present paper we studied some features of spherically symmetric two-phase deformations within the framework of phase transition zones, using a solid sphere subjected to an all-round tension as an illustrative example. We showed that inclusion of the Maxwell relation leads to a free-boundary problem. Since the conditions at the interface only depend on the material parameters, we have used a semi-inverse approach: assume the location of the interface and then determine the required boundary conditions. We showed that all equilibrium spherically symmetric two-phase deformations can be presented on a single curve determined by properties of the strain energy function, and described some general properties of the solution.

We considered two different nonlinear elastic materials in order to demonstrate a variety of phase transformation behaviours as well as some common features. For each material we showed that there were two solutions corresponding to phase transformations, that in each solution there could be only one interface, and that both two-phase deformations were energetically preferable to the one-phase deformation when radial displacement is prescribed at the external surface. Both solutions were stable with respect to perturbations of the interface radius.

We constructed phase transition zones for both materials and studied the relation between various two-phase deformations and the PTZ. In doing so we identified two kinds of deformation fields: deformation fields that are entirely outside or on the external PTZ boundary and deformation fields some parts of which are inside the internal and thus inside the external PTZ boundary. We found that deformation fields of the second kind were unstable. Although we did not find instability for deformation fields of the first kind, the question concerning the relationship between the PTZ and stability remains open. In this context we refer to the recent paper by Šilhavy (2004) where the phase transition zone is related to the notion of the quasiconvex hull of the strain energy function.

We have demonstrated the usefulness of the PTZ in characterizing the interface and the associated two-phase deformations that can appear under various loading conditions.

Acknowledgements

The authors thank the referees for their comments, which have led to improvements in the presentation of the paper. This work is supported by a Royal Society Joint Project Grant, INTAS (Grant No. 03-55-1172) and RFBR (Grant No. 04-01-0431).

References

Abeyaratne, R., 1981. Discontinuous deformation gradients in the finite twisting of an incompressible elastic tube. J. Elasticity 11, 43–80.

Abeyaratne, R., 1983. An admissibility condition for equilibrium shocks in finite elasticity. J. Elasticity 13, 175–184.

Abeyaratne, R., Bhattacharya, K., Knowles, J.K., 2001. Strain-energy functions with multiple local minima: modeling phase transformations using finite thermoelasticity. In: Fu, Y., Ogden, R.W. (Eds.), Nonlinear Elasticity: Theory and Application. Cambridge University Press, pp. 433–490.

Eremeyev, V.A., Zubov, L.M., 1991. On the stability of equilibrium of nonlinear elastic bodies with phase transformations. Mech. Solids (Izvestia AN SSSR, Mekhanika Tverdogo Tela), 56–65.

Eremeyev, V.A., Freidin, A.B., Sharipova, L.L., 2002. On nonuniqueness and stability of centrally symmetric two phase deformations. In: Proceedings of the XXIX Summer School "Advanced Problems in Mechanics" (APM2002), St. Petersburg, IPME RAS, pp. 73–83.

Eremeyev, V.A., Freidin, A.B., Sharipova, L.L., 2003. Nonuniqueness and stability in problems of equilibrium of elastic two-phase bodies. Doklady Phys. (from Doklady Akademii Nauk) 48 (7), 359–363.

Eremeyev, V.A., Freidin, A.B., Sharipova, L.L., in press. On stability of equilibrium two-phase elastic bodies. Journal of Applied Mathematics and Mechanics.

Ericksen, J.L., 1975. Equilibrium of bars. J. Elasticity 5, 191–201.

Eshelby, J.D., 1951. The force on an elastic singularity. Philos. Trans. Roy. Soc. A 244, 87–111.

Eshelby, J.D., 1956. The continuum theory of lattice defects. Solid State Physics, vol. 3. Academic Press, New York, pp. 79–144.

Eshelby, J.D., 1975. The elastic energy–momentum tensor. J. Elasticity 5, 321–335.

Fosdick, R.L., Hertog, B., 1989. The Maxwell relation and Eshelby's conservation law for minimizers in elasticity theory. J. Elasticity 22, 193–200.

Fosdick, R.L., James, R.D., 1981. The elastica and the problem of pure bending for a non-convex stored energy function. J. Elasticity 11, 165–186.

Fosdick, R.L., MacSithigh, G., 1983. Helical shear of an elastic, circular tube with a non-convex stored energy. Arch. Rational Mech. Anal 84, 31–53.

Fosdick, R.L., Zhang, Y., 1993. The torsion problem for a nonconvex stored energy function. Arch. Rational Mech. Anal. 122, 291–322.

Fosdick, R.L., Zhang, Y., 1994. Coexistent phase mixtures in the antiplane shear of an elastic tube. ZAMP 45, 202–244.

Fosdick, R.L., Zhang, Y., 1995a. A structured phase transition for the antiplane shear of an elastic circular tube. Q. J. Mech. Appl. Math. 48, 189–210.

Fosdick, R.L., Zhang, Y., 1995b. Stress and the moment-twist relation in the torsion of a cylinder with a nonconvex stored energy function. ZAMP 46, 146–171.

Freidin, A.B., 1997. Heterogeneous deformation of elastic solids due to multiple appearance of new phase layers. In: Proceedings of the 1st International Seminar "Actual Problems of Strength", 15–18 October 1997, Novgorod, Russia, vol. 1, pp. 236–240 (in Russian).

Freidin, A.B., 2000. On phase equilibrium in nonlinear elastic materials. Nonlinear problems of continuum mechanics. Izvestia Vuzov. North-Caucasus region. Special Issue, pp. 150–168 (in Russian).

Freidin, A.B., Chiskis, A.M., 1994a. Phase transition zones in nonlinear elastic isotropic materials. Part 1: Basic relations. Mech. Solids (Izvestia RAN, Mekhanika Tverdogo Tela) 29 (4), 91–109.

Freidin, A.B., Chiskis, A.M., 1994b. Phase transition zones in nonlinear elastic isotropic materials. Part 2: Incompressible materials with a potential depending on one of deformation invariants. Mech. Solids (Izvestia RAN, Mekhanika Tverdogo Tela) 20 (5), 46–58.

Freidin, A.B., Sharipova, L.L., 2003. Equilibrium two-phase deformations and phase transitions zones within framework of small strains, Nonlinear problems of continuum mechanics. Izvestia Vuzov. North-Caucasus region, pp. 291–299 (in Russian).

Freidin, A.B., Sharipova, L.L., in press. On a model of heterogenous deformation of elastic bodies by the mechanism of multiple appearances of new phase layers. Meccanica.

Freidin, A.B., Vilchevskaya, E.N., 2002. Phase transition zones for one class of nonlinear elastic materials. In: Proceedings of the XXIX Summer School "Actual Problems in Mechanics" (APM 2002), St. Petersburg, IPME RAS, pp. 43–44.

Freidin, A.B., Vilchevskaya, E.N., Sharipova, L.L, 2002. Two-phase deformations within the framework of phase transition zones. Theor. Apll. Mech., 28–29.

Fu, Y.B., Brookes, D.W., in press. An explicit expression for the surface-impedance tensor of a generally anisotropic compressible elastic material in a state of plane strain. IMA J. Appl. Math.

Fu, Y.B., Freidin, A.B., 2004. Characterization and stability of two-phase piecewise-homogeneous deformations. Proc. Roy. Soc. Lond. A 460, 3065–3094.

Grinfeld, M.A., 1980. On conditions of thermodynamic equilibrium of the phases of a nonlinear elastic material. Dokl. Acad. Nauk SSSR 251, 824–827.

Gurtin, M.E., 1983. Two-phase deformations of elastic solids. Arch. Rat. Mech. Anal. 84, 1–29.

Idesman, A.V., Levitas, V.I., Preston, D.L., Cho, J.-Y., 2004. Finite element simulations of martensitic phase transitions and microstructures based on a strain softening model. J. Mech. Phys. Solids 53, 495–523.

James, R.D., 1979. Co-existent phases in the one-dimensional static theory of elastic bars. Arch. Rat. Mech. Anal. 72, 99–140.

James, R.D., 1981. Finite deformation by mechanical twinning. Arch. Rat. Mech. Anal. 77, 143–177.

Kaganova, I.M., Roitburd, A.L., 1987. Defects heredity and the phase transformation development in solids. Sov. Phys. Solid State 29, 800–803.

Kaganova, I.M., Roitburd, A.L., 1988. Equilibrium of elastically interacting phases. Sov. Physics JETP 67, 1174–1186.

Knowles, J.K., 1979. On the dissipation associated with equilibrium shocks in finite elasticity. J. Elasticity 9, 131–158.

Knowles, J.K., Sternberg, E., 1978. On the failure of ellipticity and the emergence of discontinuous deformation gradients in plane finite elastostatics. J. Elasticity 8, 329–379.

Levitas, V.I., 1997. Phase transitions in elastoplastic materials: continuum thermomechanical theory and examples of control. J. Mech. Phys. Solids, Part I: 45(6), 923–947; Part II: 45(7), 1203–1222.

Levitas, V.I., 2000. Structural changes without stable intermediate state in inelastic material. Int. J. Plasticity 16, Part I: 805–849; Part II: 851–892.

Levitas, V.I., Idesman, A.V., Preston, D.L., 2004. Microscale simulation of martensitic microstructure evolution. Phys. Rev. Lett. 93, 105701.

Lusk, M., 1994. On martensitic phase nucleation with surface effects. J. Mech. Phys. Solids 42 (2), 241–282.

Morozov, N.F., Freidin, A.B., 1998. Phase transition zones and phase transformations in elastic bodies under various stress states. Proc. Steklov Math. Inst. 223, 219–232.

Morozov, N.F., Nazyrov, I.R., Freidin, A.B., 1996. One-dimensional problem on phase transformation of an elastic sphere. Dokl. Akad. Nauk 346, 188–191.

Nazyrov, I.R., Freidin, A.B., 1998. Phase transformation of deformable solids in a model problem on an elastic sphere. Mech. Solids (Izvestia RAN, Mekhanika Tverdogo Tela) 33 (5), 52–71.

Roitburd, A.L., Temkin, D.E., 1986. Plastic deformation and thermodynamic hysteresis at phase transformations in solids. Sov. Phys. Solid State 28, 432–436.

Rosakis, P., 1990. Ellipticity and deformations with discontinuous gradients in finite elastostatics. Arch. Rat. Mech. Anal. 109, 1–37.

Sivaloganathan, J., 1986. Uniqueness of regular and singular equilibria for spherically symmetric problems of nonlinear elasticity. Arch. Rat. Mech. Anal. 96, 97–136.

Šilhavy, M., 2004. Energy minimization for isotropic nonlinear elastic bodies. In: Del Piero, G., Owen, D.R. (Eds.), Multiscale Modeling in Continuum Mechanics and Structured Deformations. CISM International Centre for Mechanical Sciences. Courses and Lectures, 447.

Truskinovsky, L., 1982. Equilibrium interphase boundaries. Dokl. Acad. Nauk SSSR 265, 306–310.

Wang, Y., Aron, M., 1996. A reformulation of the strong ellipticity conditions for unconstrained hyperelastic media. J. Elasticity 44, 89–96.